Charge-charge interaction in three-layer systems: Classical approach

Alexander M. Gabovich [1,*] Mai Suan Li [2,†] Henryk Szymczak [2,‡] and Alexander I. Voitenko [1,§]

[1] *Institute of Physics, National Academy of Sciences of Ukraine, 46 Nauky Ave., Kyiv 03680, Ukraine*

[2] *Institute of Physics, Polish Academy of Sciences, 32/46 Al. Lotników, PL-02-668 Warsaw, Poland*

(Received 10 January 2022; revised 24 February 2022; accepted 2 March 2022; published 15 March 2022)

General explicit analytical expressions for the charge-charge interaction energy $W(Z, Z', R)$ between two point charges in heterostructures with three plane layers were obtained in the framework of classical electrostatics, i.e., the dielectric permittivities of the constituent media were assumed to be constant. Here, R is the lateral (along the interfaces) distance between the charges, and Z and Z' are their normal coordinates. The obtained results may be applied to the interaction between charges for their various arrangements in the layered system. For instance, the interaction across the interlayer was calculated as the function of the dielectric constants ε_i ($i = 1, 2, 3$) of the constituent media. It was demonstrated that the textbook Coulomb expression is far from being valid in this case. In particular, more sophisticated formulas proposed here should be used when considering interlayer excitons in heterostructures of various kinds and electron-hole superfluidity in such sandwiches.

DOI: 10.1103/PhysRevB.105.115415

I. INTRODUCTION

The availability of a comprehensive theory describing the electrostatic charge interaction in three-layered systems is important for a number of problems in condensed matter physics, electrochemistry, and biophysics. Among those issues, it is worth mentioning, first of all, the determination of binding energy [1–16] and the calculation of the quantum or dielectric confinement [7,9,17–27] of intralayer excitons and trions. In such cases, the electron (hole) subsystem in any layer is often assumed to be close to the limiting two-dimensional (2D) configuration [28–31] so that the lateral distance R between the exciton constituents (the electron and the hole) is much larger than the interlayer width L. Then, the famous Rytova-Keldysh approximation [1,32] for the charge-charge interaction is applied, which is not always valid (see our previous work [33]). On the other hand, studies of the interlayer excitons in dichalcogenide heterostructures, where a vertical geometry of the electron-hole complex is most energetically beneficial, have been started recently [34–37]. Therefore, R may be equal to zero so that the Rytova-Keldysh simplification fails from the outset and a more general treatment of the problem concerned is required.

There are also other problems where the knowledge of Coulomb interaction in layered systems is needed. For instance, we should mention the hypothetical electron-hole superfluidity [38–42], certain surface properties studied by scanning probe spectroscopy [43,44], the behavior of suspended electron image states near the surface of materials with low dielectric constants [45–49], the arrangement of ions trapped in layered systems [47,50,51], the formation of organic self-assembled monolayers on metal substrates [52], as well as the electrostatic aspects of biologically important molecules and multimolecular assemblies [53–56].

A number of attempts were made to solve the problem of electrostatic charge interaction in two-layer, three-layer, and even multilayer systems. The majority of the productive theories dealing with this interaction used the simple approximation of sharp interfaces between the media involved, with each medium described by its own bulk dielectric function $\varepsilon_i(\mathbf{k}, \omega)$, where the subscript i marks the layer, and $\mathbf{k}$ and ω mean the transferred wave vector and frequency, respectively (below we will equally identify $\mathbf{k}$ and ω with the transferred momentum and energy by putting the Planck constant $\hbar = 1$) [3,4,57–67]. The medium constituent charge carriers are most often considered as specularly reflected at layer boundaries, although other types of the carrier behavior near the layer surfaces were also studied and led to similar results. It is remarkable that the macroscopic description [68–76] of the response of a conducting or insulating medium in terms of the function $\varepsilon(\mathbf{k}, \omega)$ [the tensor $\varepsilon_{\alpha\beta}(\mathbf{k}, \omega)$ for anisotropic substances [76,77]] can be successfully applied even to one-layer materials such as graphene and its derivatives [29,78–84]. Of course, the problems for three-layer and multilayer systems are much more involved than in the case of two layers. The difficulty consists in the necessity of taking into account an infinite sequence of images if the number of interfaces is larger than two [85–90]. In this paper, we will mainly deal with three-layer systems, using the two-layer system as a reference point.

Two charges in a three-layer system not only interact with each other but also polarize the interfaces between the layers and interact with the emerging polarization charges. As a result, the total electrostatic energy of the system equals

$$W_{\text{tot}} = W_{\text{int}} + W_{\text{im}} + W'_{\text{im}}. \tag{1}$$

*gabovich@iop.kiev.ua
†masli@ifpan.edu.pl
‡szymh@ifpan.edu.pl
§voitenko@iop.kiev.ua

 ©2022 American Physical Society

Here, the summands $W_{\rm im}$ and $W'_{\rm im}$ describe the image force energies for each of the charges. If the charged entities do not modify the screening properties of the media (for instance, the polaronlike effects are neglected), each of those quantities depends separately on the coordinates of the relevant charge in the system. Therefore, sometimes they are quite reasonably called self-energy terms [6,87,91]. The self-terms were extensively studied by us earlier [92], so they are not touched upon in this paper. At the same time, $W_{\rm int}$ depends on the coordinates of both charges and suffers the influence of the polarization charges as well because each charge interacts not only with its counterpart, but also with the polarization charges induced by the latter at both interfaces. It is the quantity $W_{\rm int}$, which is the genuine charge-charge interaction and will be denoted as W below, is the matter of concern and will be discussed here in detail. The emphasis will be mainly made on the displacement of the charges directed normally (the Z axis) to the interface since their interaction at their identical vertical positions in three-layer structures ($Z = Z'$) and the varying distance along the interfaces has been already considered by us earlier [33] in the context of the exciton formation in almost two-dimensional layers [11–13,21,36,93]. Nevertheless, the formulas obtained now contain the full kit of problem parameters including the charges' coordinates without any restrictions on the latter. Therefore, they present the general solution of the formulated problem.

The general calculation scheme is valid for arbitrary physically justified functions $\varepsilon_i(\mathbf{k}, \omega)$. Nevertheless, analytical and numerical calculations were performed in the classical electrostatic approximation for each layer: $\varepsilon_i(\mathbf{k}, \omega) = \varepsilon_i = \text{const}$ [85,94]. It allowed us to derive the general solution in the form of exact analytical formulas. The results obtained can be considered as a useful guide at least for wide-gap semiconductors, although they are valid even if one of the layers is metallic or ferroelectric ($\varepsilon_i \to \infty$).

The outline of the paper is as follows. The concise formulation of the problem, the calculation results in the classical electrostatic approximation (ε_i's are constants, $i = 1, 2, 3$), and their interpretation in the framework of the image-charge scenario are described in Sec. II. In Sec. III, a particular case, which is important for the problem of formation of interlayer excitons and treating the charge-charge interaction across the interlayer is analyzed. Section IV is devoted to various simplifying approximations, which allowed us to obtain simple expressions for the interaction between charges located arbitrarily in the heterostructure. Appendixes A and B contain full sets of formulas in the general and classical electrostatic cases, respectively.

II. FORMULATION AND RESULTS OF CALCULATIONS

A. Charge-charge interaction in three-layer structures in the classical electrostatic approach

Let us consider a three-layer system (see Fig. 1) composed of classically described homogeneous nondispersive insulators with dielectric constants $\varepsilon_i = \text{const}$, $i = 1, 2, 3$. The slab ($i = 2$) is a plane-parallel layer of thickness L located in-between two semi-infinite covers ($i = 1, 3$). We choose a Cartesian coordinate frame (X, Y, Z) with the Z axis directed

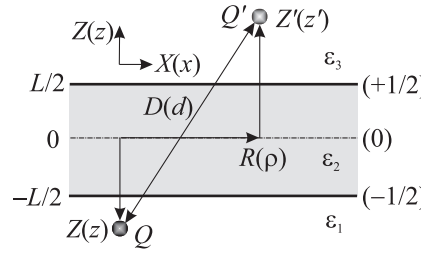

FIG. 1. Arrangement of the charges Q and Q' in a three-layer plane heterostructure. The width of interlayer 2 (slab) is L. Layers 1 and 3 (covers) are semi-infinite. ε_i ($i = 1, 2, 3$) are dielectric constants of the corresponding layers. Dimensional quantities are denoted by capital letters, dimensionless quantities normalized by L are denoted by lowercase letters and in parentheses. The coordinate Z (or z) is normal to the interfaces, and the coordinate X (or x) is parallel to them. The coordinate Z is reckoned from the middle of the interlayer. D (or d) is the distance between the charges, whereas R (or $\rho = R/L$) is the lateral distance between them.

perpendicularly to the interfaces between the media and the XY plane ($Z = 0$) being the midplane of the slab. Then, the plane and infinitesimally thin interfaces between media 1 and 2 and between media 2 and 3 are the planes $Z = -L/2$ and $Z = L/2$, respectively. The system is invariant with respect to translations in the XY plane.

It should be recognized that this approach neglects the atomic structure of both interfaces and implies that the latter are sharp and separate the media described by their bulk properties (in our case, each medium is represented exclusively by its bulk dielectric constants). Thus, our approach corresponds to the classical electrostatic limit of the more general infinite-barrier model (IBM) [67,95–100] (in classical electrostatics, the difference disappears between the genuine IBM, where Friedel oscillations of the electron gas density [101] are induced due to the electron gas perturbation by the lattice truncation at the surface, and the even simpler semiclassical IBM [102,103], where such oscillations are absent). In both those models, the condensed matter media divided by the interfaces are described by their bulk dielectric functions $\varepsilon_i(\mathbf{k}, \omega)$.

Two point charges Q and Q' are embedded into the heterostructure. They have the normal coordinates Z and Z', respectively, and are separated by the lateral (along the interfaces) distance R. Our aim is to calculate the energy of electrostatic interaction W between those charges and its dependence $W(\{\varepsilon\}, Z, Z', R)$ on the problem parameters, where the notation $\{\varepsilon\} = \{\varepsilon_1 : \varepsilon_2 : \varepsilon_3\}$ means the set of corresponding dielectric constants. The heterostructure (without the charges) is characterized by a single length parameter, the interlayer width L. Such a simplicity makes it possible and convenient, in what follows, to use L as a normalizing parameter and change to the dimensionless coordinates

$$z^{(\prime)} = Z^{(\prime)}/L, \quad \rho = R/L$$

and the dimensionless interaction energy (the $\{\varepsilon\}$ dependence is implied)

$$w(z, z', \rho) = \left(\frac{QQ'}{L}\right)^{-1} W(\{\varepsilon\}, Z, Z', R). \tag{2}$$

Appendix A contains a more general analytical formulation of the problem, where the spatial and temporal dispersion of the dielectric permittivities for all constituent media are taken into account. Whereas the account of the spatial dispersion of dielectric permittivity makes further calculations very cumbersome, the temporal dispersion is formally easier to be incorporated into the general scheme. Then, the plasmon spectrum in three-layer systems can be obtained. However, this task, being very important, e.g., for systems including graphene layers [104], goes far beyond the electrostatic problems studied here.

The solution obtained in the considered case of classical homogeneous nondispersive insulators (see Appendix B) is presented below. It is written in the form that satisfies the following, obvious for the classical electrostatic system, symmetry conditions (we recall that the self-image forces are not considered in this paper):

(i) the interaction energy has to be insensitive to the sign of ρ,

$$w(\{\varepsilon\}, z, z', \rho) = w(\{\varepsilon\}, z, z', -\rho); \tag{3a}$$

(ii) the permutation of the charges cannot change the expression for $w(\{\varepsilon\}, z, z', \rho)$, irrespective of the media where the charges are located,

$$w(\{\varepsilon\}, z, z', \rho) = w(\{\varepsilon\}, z', z, \rho); \tag{3b}$$

hence, the difference $z - z'$ can enter only as its absolute value $|z - z'|$;

(iii) the specular reflection of the system with respect to the plane $z = 0$ (the notation "$^-$" so that $\bar{z} = -z$, $\bar{z}' = -z'$, and $\{\bar{\varepsilon}\} = \{\varepsilon_3 : \varepsilon_2 : \varepsilon_1\}$) also cannot change the interaction energy:

$$w(\{\varepsilon\}, z, z', \rho) = w(\{\bar{\varepsilon}\}, -z, -z', \rho). \tag{3c}$$

Note that if the configuration is symmetric, i.e., $\varepsilon_1 = \varepsilon_3$, we have $\{\varepsilon\} = \{\bar{\varepsilon}\}$ and condition (3c) looks like

$$w(\{\varepsilon\}, z, z', \rho) = w(\{\varepsilon\}, -z, -z', \rho). \tag{3c+}$$

As a result, in the symmetric case, the sum $z + z'$ can also be included inside the absolute value brackets $|z + z'|$.

The solution of the posed problem consists of several branches depending on the distribution of the charges among the layers. To shorten further expressions, it is convenient to employ the following enumeration for the media:

$$\mathrm{med}(z) = \begin{cases} 1 & \text{if } z \leqslant -\frac{1}{2}, \\ 2 & \text{if } -\frac{1}{2} < z < \frac{1}{2}, \\ 3 & \text{if } z \geqslant \frac{1}{2}, \end{cases} \tag{4}$$

and use the notation $w_{ij}(z, z')$ (the $\{\varepsilon\}$ set and the lateral distance ρ are omitted from the arguments) to describe the interaction energy (2) in the case when $\mathrm{med}(z) = i$ and $\mathrm{med}(z') = j$, i.e., when one of the charges is in the ith and the other in the jth layer. Now, making use of the notations Λ and λ_{ij} introduced in Appendix B, some branches $w_{ij}(z, z')$ of the final solution can be written via function (B11) as follows (the arguments Λ and ρ in the Ξ functions are omitted for brevity):

$$w_{33}(z, z') = \frac{1}{\varepsilon_3}[\Xi(|z - z'|) + \Lambda\,\Xi(|z - z'| + 2) - \lambda_{12}\,\Xi(|z + z'| + 1) - \lambda_{23}\,\Xi(|z + z'| - 1)], \tag{5}$$

$$w_{32}(z, z') = \frac{2}{\varepsilon_2 + \varepsilon_3}[\Xi(|z - z'|) - \lambda_{12}\,\Xi(|z + z'| + 1)], \tag{6}$$

$$w_{31}(z, z') = \frac{4\varepsilon_2}{(\varepsilon_1 + \varepsilon_2)(\varepsilon_2 + \varepsilon_3)}\,\Xi(|z - z'|). \tag{7}$$

Owing to the problem and, hence, solution symmetries, the other components (these are w_{11}, w_{12}, w_{13}, w_{21}, and w_{23}) can be derived on the basis of the following reasoning. All those expressions must and do satisfy the relationship $w_{ij}(z, z') = w_{ij}(z', z) \equiv w_{ji}(z, z')$, i.e., the interaction energy of two charges remains invariant if we interchange the charge positions [condition (ii)]. Thus, $w_{13}(z, z') = w_{31}(z, z')$ and $w_{23}(z, z') = w_{32}(z, z')$. The formula for w_{12} (the charge Q is in medium 1 and the charge Q' in medium 2) can be obtained from expression (6) (the charge Q is in medium 3 and the charge Q' in medium 2) in two steps: (i) we change $z \to -z$ and $z' \to -z'$ in formula (6), which corresponds to the reflection of the system with respect to the central plane $z = 0$; (ii) then we change $\varepsilon_1 \leftrightarrow \varepsilon_3$, i.e., restore media 1 and 3 at their initial locations. The expression for $w_{11}(z, z')$ can be derived analogously. In doing those transformations, one should bear in mind that $|z - z'| = |z' - z|$ and $|z + z'| = |-z - z'|$. As a result, we obtain

$$w_{12}(z, z') = \frac{2}{\varepsilon_2 + \varepsilon_1}[\Xi(|z - z'|) - \lambda_{32}\,\Xi(|z + z'| + 1)], \tag{8}$$

$$w_{11}(z, z') = \frac{1}{\varepsilon_1}[\Xi(|z - z'|) + \Lambda\,\Xi(|z - z'| + 2) - \lambda_{32}\,\Xi(|z + z'| + 1) - \lambda_{21}\,\Xi(|z + z'| - 1)]. \tag{9}$$

The situation with the expression of the w_{22} branch,

$$w_{22}(z, z') = \frac{1}{\varepsilon_2}\{\Xi(|z - z'|) - \Lambda\,\Xi(2 - |z - z'|) + \lambda_{21}\,\Xi[1 + (z + z')] + \lambda_{23}\,\Xi[1 - (z + z')]\}, \tag{10}$$

is more interesting. We should not write $|z + z'|$ in the last two terms. Otherwise, we should introduce two subbranches where those terms would interchange their coefficients.

In Eqs. (5)–(10), as well as in other branch expressions, there are four groups of terms. The terms of the first group are proportional to $\Xi(|z - z'|)$. If the charges are located in the same medium [see Eqs. (5) and (10)], those terms contain a coefficient inverse to the dielectric permittivity of the medium. In such a case, this term can be attributed to the direct interaction between the charges, whereas the other terms in the expression describe the charge interaction with polarization charges. But if the charges are in different media [see Eqs. (6) and (7)], the situation is more complicated. The plane geometry, e.g., of the 3-2 interface [see Eq. (6)] makes it impossible for the charge Q' located in medium 2 to functionally distinguish between its interaction with the charge Q located in medium 3 and with the polarization charge created by the charge Q at the 3-2 interface. As a result, both contributions

are summed up to produce a term with an "effective dielectric permittivity" so that it cannot be attributed to the direct charge interaction alone. This circumstance can be especially clearly seen from expression (7) for the w_{31} branch, where every component of the interaction, e.g., of the charge Q' in medium 1 with (a) the charge Q in medium 3, (b) with the polarization charge induced by the charge Q at the 1-2 interface, and (c) with the polarization charge induced by the charge Q at the 2-3 interface has the identical functional dependence on the spatial parameters and there are no other components. The situation is analogous to that arising in the two-layer configuration [see Eq. (12) below].

The terms of the second group are proportional to $\Xi(|z+z'|+1)$ or $\Xi[1+(z+z')]$. They are generated by the polarization of the 1-2 interface. The third group of terms contains the functions $\Xi(|z+z'|-1)$ and $\Xi[1-(z+z')]$, which are generated by the 2-3 interface. The contributions of the terms in those two groups contain the relevant factor ($\lambda_{12}=-\lambda_{21}$ or $\lambda_{23}=-\lambda_{32}$) in the same manner as the direct term. Finally, there is the fourth group of terms which are proportional to $\Xi(|z-z'|+2)$ or $\Xi(2-|z-z'|)$. They reflect the interference between the image charges arising at both interfaces [85–90]. That is why the parameter Λ appears in them as a factor. All terms are very simple, which allows a straightforward interpretation (see Sec. II C) and a relatively easy treatment.

The obtained expressions represent the general solution of the electrostatic problem concerned and, to our knowledge, have not been obtained earlier. They satisfy all limiting cases. In particular, it is easy to verify that they correctly describe the two-layer problem. For instance, if, e.g., $\varepsilon_2=\varepsilon_3$, i.e., both charges are in the same cover 3 adjacent to cover 1, then formulas (5), (6), and (10) look like ($\Lambda=\lambda_{23}=0$)

$$w_{33}(z,z')=\frac{1}{\varepsilon_3}\frac{1}{\sqrt{\rho^2+(z-z')^2}}-\frac{\lambda_{13}}{\varepsilon_3}\frac{1}{\sqrt{\rho^2+(z+z'+1)^2}}, \tag{11}$$

i.e., the interaction energy contains a direct term and an image-force-related one, whereas formula (7) reads as

$$w_{31}(z,z')=\frac{2}{\varepsilon_1+\varepsilon_3}\frac{1}{\sqrt{\rho^2+(z-z')^2}}, \tag{12}$$

as it should be in the classical case [85], i.e., the direct and indirect contributions to the interaction energy become indiscernible.

Formula (5) contains two pairs of Ξ functions, with the arguments in each pair differing by 2. Therefore, according to formulas (B12) and (B13), we can reduce the number of Ξ functions. In particular, the application of formula (B13) results in

$$w_{33}(z,z')=\frac{1}{\varepsilon_3}\frac{1}{\sqrt{\rho^2+(z-z')^2}}-\frac{\varepsilon_2+\varepsilon_3}{\varepsilon_3(\varepsilon_2-\varepsilon_3)}\frac{1}{\sqrt{\rho^2+(z+z'-1)^2}}+\frac{4\varepsilon_2}{(\varepsilon_2^2-\varepsilon_3^2)}\Xi(z+z'-1) \tag{13}$$

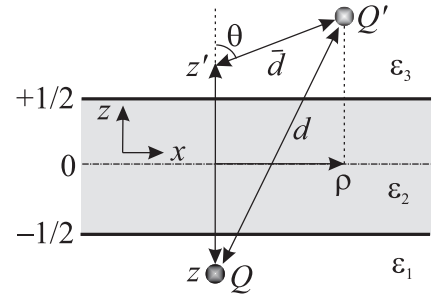

FIG. 2. The same as in Fig. 1, but with the indication of the auxiliary quantity $\bar{d}$, which is the distance of the charge Q' from the point $(0,0,z')$. The angle θ ($-\frac{\pi}{2}\leqslant\theta\leqslant\frac{\pi}{2}$) is the angle between the axis z and the segment $\bar{d}$.

so that only a single Ξ function survives. This formula makes it easy to see that if the charges retain their relative arrangement ($\rho=$ const and $z-z'=$ const) and hence their relative distance

$$d=\sqrt{\rho^2+(z-z')^2}, \tag{14}$$

but move into the depth of cover 3 [i.e., $(z,z')\to\infty$], then $w_{33}(z,z')$ tends to its first summand, which describes the textbook charge interaction in an infinite medium with the dielectric permittivity ε_3.

Nevertheless, formula (13) provokes a serious concern because two of its terms contain the difference $\varepsilon_2-\varepsilon_3$ in the denominator. If $\varepsilon_2\to\varepsilon_3$, we should apply formula (B12) once more to obtain

$$w_{33}(z,z')=\frac{1}{\varepsilon_3}\frac{1}{\sqrt{\rho^2+(z-z')^2}}-\frac{\varepsilon_2-\varepsilon_3}{\varepsilon_3(\varepsilon_2+\varepsilon_3)}\frac{1}{\sqrt{\rho^2+(z+z'-1)^2}}-\frac{4\varepsilon_2}{(\varepsilon_2+\varepsilon_3)^2}\frac{\varepsilon_1-\varepsilon_2}{(\varepsilon_1+\varepsilon_2)}\Xi(z+z'+1). \tag{15}$$

Thus, in actual fact, the apparent divergences in Eq. (13) mutually cancel out, resolving the problem.

Let us consider the long-range asymptotics of expressions (5)–(7). Let the charge Q be fixed in the ith medium at the point $(0,0,z)$, and the charge Q' be in medium 3, in the xz plane, at the distance $\bar{d}$ from the point $(0,0,z')$ (see Fig. 2).

Then, the coordinates of the charge Q' are $(\bar{d}\sin\theta,0,z'+\bar{d}\cos\theta)$, where θ is the angle between the normal to the slab and the segment connecting the charge Q' with the point $(0,0,z')$ ($-\frac{\pi}{2}\leqslant\theta\leqslant\frac{\pi}{2}$). It turns out that in all three cases $i=1,2,3$ [see definition (2)], i.e., irrespective of where the charge Q is located, and irrespective of the angle θ (the only restriction on $\bar{d}$ and θ is that the charge Q' should reside in medium 3), we have

$$\lim_{\bar{d}\to\infty} w_{3i}(z+\bar{d}\cos\theta,z',\rho=\bar{d}\sin\theta)=\frac{2}{\varepsilon_1+\varepsilon_3}\frac{1}{d}+O(d^{-2}). \tag{16}$$

The same result is obtained if operating with d rather than $\bar{d}$ in the left-hand side of Eq. (16), but the intermediate calculations are more cumbersome. In essence, we come once

more to the expression on the right-hand side of two-layer formula (12). On the other hand, the same limit (16) is also obtained for $d \to \infty$ from Eq. (11). It is remarkable that the slab parameters ε_2 and L (the latter as the unity in linear combinations with z and z') are not present in this expression. Of course, we will obtain the same result if we move the charge Q' over medium 3 far from the charge Q fixed in any of the media. It looks like the charges, when being located at rather long (as compared with the interlayer width) distances from each other, cease to perceive the presence of the slab. To explain this result, let us normalize all the problem lengths by $\bar{d}$ rather than the slab width. Then, as $\bar{d}$ grows, (i) the newly normalized slab width vanishes, (ii) the slab itself transforms into an interface between covers 1 and 3, and (iii) either one of the charges (in the scenario above with $\theta \neq \frac{\pi}{2}$, this is the charge Q with the fixed z coordinate) or both of them (this is the scenario with $\theta = \frac{\pi}{2}$ so that the charge Q' moves laterally and its z coordinate also remains fixed) settle on this interface. Thus, we obtain a two-layer configuration described by the expression in the right-hand side of Eq. (12) with $z' = 0$.

On the other hand, if the charges approach each other ($\rho \to 0$ and $z' \to z$) close enough, the zeroth term (equal to d^{-1}) in $\Xi(|z - z'|)$ begins to prevail in every branch $w_{ij}(z, z')$. Then

$$w_{ii}(z \to z', \rho \to 0) \to \frac{1}{\varepsilon_i d} \tag{17}$$

in each medium ($i = 1$–3) and

$$w_{ij}(z \to z', \rho \to 0) \to \frac{2}{(\varepsilon_i + \varepsilon_j)d} \tag{18}$$

across each interface (1-2 or 2-3). Only the nearest vicinity of the charges is important and the charges interact like in the corresponding infinite medium [formula (17)] or across the interface in a two-layer one [formula (18)]. At the same time, if, e.g., we put $z = \frac{1}{2}$ in expression (5) or (13) from the very beginning, then the passage to the limit ($\rho \to 0, z' \to \frac{1}{2}$) will give result (18) rather than (17). Thus, we obtain a "double jump" across each interface.

However, such a discontinuity takes place only in the case $\rho \to 0$. Otherwise ($\rho \neq 0$), the w_{ij} branches transform continuously if any of the coordinates z and z' any of the interfaces, i.e.,

$$\lim_{z,z' \to \pm\frac{1}{2} - 0} w(z, z', \rho \neq 0) = \lim_{z,z' \to \pm\frac{1}{2} + 0} w(z, z', \rho \neq 0). \tag{19}$$

Therefore, the charge, e.g., at the ($z = \frac{1}{2}$) interface cannot be ascribed either to medium 2 or to medium 3 (bear in mind that we are in the frame of the model with infinitely thin interfaces!). However, calculations with the basic functions a_S and a_A may be more cumbersome in comparison to those with their a_1 and a_3 counterparts (see Appendix B) so that identification (4) was made.

An interesting feature of formula (12) is that its coordinate dependence is reduced to the dependence on the distance d between the charges [formula (14)]. In other words, if the charges are not embedded into the same cover (one or both of them can even be located at the interface), only the intercharge distance d rather than the specific charge locations matters. A simple consideration testifies that formula (7) can also demonstrate such a behavior but only if the charges are located on the same normal to the interfaces, i.e., if their lateral distance equals zero, $\rho = 0$. In this case, the intercharge distance equals $|z - z'|$.

Note that the "normal" arrangement of the charges ($\rho = 0$) is rather important for applications (see Sec. III). Then, the function Ξ is reduced to the tabulated Lerch transcendent Φ [see formula (B14)]. In this case, Eqs. (5)–(10) look like

$$\begin{aligned} w_{33}(z, z', \rho = 0) = \frac{1}{2\varepsilon_3}\Bigg\{ & \Phi\left[-\Lambda, 1, \frac{|z - z'|}{2}\right] \\ & + \Lambda\Phi\left[-\Lambda, 1, \frac{|z - z'| + 2}{2}\right] \\ & - \lambda_{12}\Phi\left[-\Lambda, 1, \frac{|z + z'| + 1}{2}\right] \\ & - \lambda_{23}\Phi\left[-\Lambda, 1, \frac{|z + z'| - 1}{2}\right]\Bigg\}, \end{aligned} \tag{20}$$

$$\begin{aligned} w_{32}(z, z', \rho = 0) = \frac{1}{(\varepsilon_2 + \varepsilon_3)}\Bigg\{ & \Phi\left[-\Lambda, 1, \frac{|z - z'|}{2}\right] \\ & - \lambda_{12}\Phi\left[-\Lambda, 1, \frac{|z + z'| + 1}{2}\right]\Bigg\}, \end{aligned} \tag{21}$$

$$\begin{aligned} & w_{31}(z, z', \rho = 0) \\ & = \frac{2\varepsilon_2}{(\varepsilon_1 + \varepsilon_2)(\varepsilon_2 + \varepsilon_3)}\left\{\Phi\left[-\Lambda, 1, \frac{|z - z'|}{2}\right]\right\}, \end{aligned} \tag{22}$$

$$\begin{aligned} w_{11}(z, z', \rho = 0) = \frac{1}{2\varepsilon_1}\Bigg\{ & \Phi\left[-\Lambda, 1, \frac{|z - z'|}{2}\right] \\ & + \Lambda\Phi\left[-\Lambda, 1, \frac{|z - z'| + 2}{2}\right] \\ & - \lambda_{32}\Phi\left[-\Lambda, 1, \frac{|z + z'| + 1}{2}\right] \\ & - \lambda_{21}\Phi\left[-\Lambda, 1, \frac{|z + z'| - 1}{2}\right]\Bigg\}, \end{aligned} \tag{23}$$

$$\begin{aligned} w_{12}(z, z', \rho = 0) = \frac{1}{(\varepsilon_2 + \varepsilon_1)}\Bigg\{ & \Phi\left[-\Lambda, 1, \frac{|z - z'|}{2}\right] \\ & - \lambda_{32}\Phi\left[-\Lambda, 1, \frac{|z + z'| + 1}{2}\right]\Bigg\}, \end{aligned} \tag{24}$$

$$\begin{aligned} w_{22}(z, z', \rho = 0) = \frac{1}{2\varepsilon_2}\Bigg\{ & \Phi\left[-\Lambda, 1, \frac{|z - z'|}{2}\right] \\ & + \lambda_{21}\Phi\left[-\Lambda, 1, \frac{1 + (z + z')}{2}\right] \\ & + \lambda_{23}\Phi\left[-\Lambda, 1, \frac{1 - (z + z')}{2}\right] \\ & - \Lambda\Phi\left[-\Lambda, 1, \frac{2 - |z - z'|}{2}\right]\Bigg\}. \end{aligned} \tag{25}$$

Again, $w_{ji}(z, z', \rho = 0) = w_{ij}(z, z', \rho = 0)$.

B. Calculation results

The interaction of two point charges located identically ($z = z'$) within the same layer of a three-layer system was studied in detail in our previous publications [33,105]. Our results demonstrated that the famous Rytova-Keldysh

approximation [1,32] applied to present Coulomb potential in thin films, especially to calculate the exciton formation and properties [10,29,30], is overused because its range of applicability is narrower than it is sometimes assumed (see discussion in Sec. III). However, another arrangement can be realized when the charges are located in different layers or in the same layer but at different z's. In the latter case, if $R \gg L$, the results obtained in the cited works can be applicable within the allowable accuracy. But, if $R \gtrless L$, i.e., $\rho \gtrless 1$, the situation changes. For instance, such a relationship corresponds to the interlayer Wannier-Mott excitons [34–37], as well as charged colloidal particles [106–112] suspended in different layers of immiscible liquids [113–121]. This subsection is serves to illustrate the formulas obtained for the electrostatic interaction in the previous subsection.

To be specific, here we plot the $w(z, z', \rho)$ (or related, see below) dependencies when the charge Q location is assumed to be fixed ($z = \text{const}$), whereas the charge Q' is shifted ($z' = \text{var}$) perpendicularly ($\rho = \text{const}$) to the interfaces. In such a manner, it is possible to cover all kinds of relative arrangements of both charges in the layers. To illustrate the whole situation, we selected three "toy" $\{\varepsilon\}$ sets: $\{1 : 2 : 5\}$ (monotonically changing ε's), $\{2 : 1 : 5\}$ (the dielectric constant ε_2 in the slab is minimal), and $\{1 : 5 : 2\}$ (the dielectric constant ε_2 in the slab is maximal). Furthermore, we fully recognize that the classical electrostatic approach with constant dielectric permittivities may turn out to be rather crude, so one cannot expect quantitative agreement with, e.g., precise experiments on the dielectric confinement of charge carriers [7,9,17,20,23,122]. Therefore, to obtain a qualitative picture, we mainly restrict the interval of charges' z coordinates to $[-2.5, 2.5]$, i.e., the charges are not shifted away from the nearest interlayer surface ($z = \pm\frac{1}{2}$) by more than twice the slab width. Nevertheless, when describing the long-range asymptotics, this interval will be extended.

Figure 3(a) demonstrates the calculated results of the dependencies $w(z, z', \rho = 0.1)$ for the configuration $\{\varepsilon\} = \{2 : 1 : 5\}$. Namely, we selected the set $\{z\} = \{-1, -\frac{1}{2}, 0, \frac{1}{2}, 1\}$ describing the fixed positions of the charge Q in cover 1, at the cover 1–slab 2 interface, in the middle of slab 2, at the slab 2–cover 3 interface, and in cover 3, respectively. The charge Q', being at the lateral distance $\rho = 0.1$, "moves" along a normal to the slab. The plotted dependencies demonstrate rather sharp peaks when the charges approach to the minimal distance between them (when $z \to z'$), which makes it hard to notice peculiar cusps at $z' = \pm\frac{1}{2}$. Figure 3(b) is more informative. There, the dependencies $w(z, z', \rho) \times d$ are plotted for the same parameter set. Here, the factor d compensates to a great extent variations associated with the direct Coulomb interaction between the charges and makes the deviations associated with the system heterogeneity more evident. The dependencies retain qualitative information about the peak amplitude ratios (see the circles). However, now, the corresponding distinctive points can become even a minimum of the whole dependence [see the ($z = 1$) curve].

Nevertheless, in our opinion, the reciprocal combination $(wd)^{-1}$ is even a more illustrative and understandable quantity. It is so because very often the interaction energy is approximated by means of the classical Coulombic

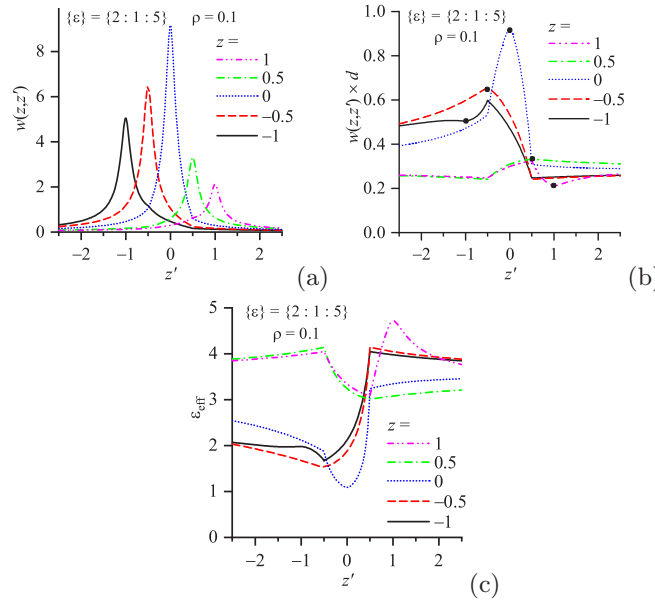

FIG. 3. (a) Dependencies of the dimensionless interaction energy $w(z, z') = W(Z, Z') \times (QQ'/L)^{-1}$ between the charges Q and Q' on the coordinate z' of the charge Q' for the lateral distance $\rho = 0.1$ and various values of the coordinate z of the charge Q. The dielectric constants of the layers are $\{\varepsilon\} = \{2 : 1 : 5\}$. Similar dependencies of $d \times w(z, z')$ and the effective dielectric permittivity $\varepsilon_{\text{eff}} = [d \times w(z, z')]^{-1}$ are displayed in (b) and (c), respectively.

dependence

$$w = \frac{1}{\varepsilon_{\text{eff}} d}, \tag{26}$$

thus introducing the effective dielectric constant ε_{eff}. Then, the quantity $(wd)^{-1}$ equals ε_{eff}, which allows a simple comparison of the results with the dielectric constants of constituting media to be made. It should be noted that in layered systems, where all three dielectric permittivities are constants ε_i ($i = 1, 2, 3$), the effective dielectric "constant" ε_{eff} is no longer a constant but depends on spatial coordinates [16,123], being in essence a nonlocal dielectric *function*. However, in certain cases, the introduction of spatially averaged true "effective dielectric constants" in such systems may also be useful [87,124,125]. Figure 3(c) depicts the dependencies $\varepsilon_{\text{eff}}(z, z', \rho)$ for the same parameter set as in Figs. 3(a) and 3(b). Note that according to formula (16), all plotted curves must tend to $\frac{1}{2}(\varepsilon_1 + \varepsilon_3)$ (in the presented configuration, this is 3.5) as $z' \to \pm\infty$. Our calculations show that this limit is achieved at such large distances from each interface that it might be considered as the quantity of academic interest. However, its existence is important from the principal viewpoint and proves the validity of the whole approach adopted here. One can also easily see that the parameter ε_{eff} changes rather strongly across the heterostructure, so that the very concept of the effective dielectric *constant* is vague, whereas the dielectric *function* $\varepsilon_{\text{eff}}(z, z', \rho)$, although being *per se* a loose quantity, serves as a good measure of deviations from the textbook Coulomb law whatever constant is inserted into Eq. (26). A detailed analysis of the Coulomb law modification

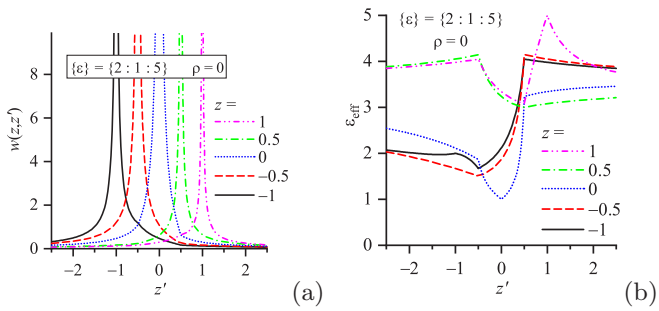

FIG. 4. The same dependencies as in Figs. 3(a) and 3(c), but for $\rho = 0$.

in two- and three-layer systems was carried out elsewhere [33,105,126].

The representation of results as $\varepsilon_{\text{eff}}(z, z', \rho)$ has an additional advantage: it demonstrates a continuity even if the w representation becomes discontinuous. In Fig. 4, analogs of Figs. 3(a) and 3(c) are shown in the extreme case $\rho = 0$, when the both charges are located on the same vertical line. At $z' \to z$, the charge Q' can approach infinitesimally close to the charge Q and the $w(z')$ dependence has a singularity [Fig. 3(a)]. This singularity effectively "obscures" other specific features associated with the system heterogeneity. But the corresponding $\varepsilon_{\text{eff}}(z')$ dependencies [Fig. 3(b)] are free of such singularities. By comparing Figs. 3(c) and 4(b), one can see that the corresponding curves are very similar to each other and smoothly transform into each other when the problem parameter (in the considered case, this is ρ) changes. Thus, the ε_{eff} dependencies can provide valuable information, which can be lost while analyzing singular w dependencies. Therefore, hereafter, we will mainly use the ε_{eff} representation to illustrate the calculation results.

Figure 5 extends the parameter scope of Fig. 3. Here, the $\varepsilon_{\text{eff}}(z, z', \rho)$ dependencies are plotted not only for $\rho = 0.1$ but for the set $\{\rho\} = \{0.1, 0.2, 0.5, 1, 2\}$. The solid curves correspond to the curves displayed in Fig. 3(c). One can see that all remarks made concerning Fig. 2(c) remain valid in this case as well.

Let us consider Fig. 4 where the charges can approach infinitesimally close to each other, once more. According to the discussion in Sec. II A [formulas (17) and (18)], if they are in the bulk of the same medium, the presence of other media, as well as the interfaces, located at finite distances from them has no matter because the singularity of direct interaction effectively wipes out any traces of the polarization charge influence. As a result, $\varepsilon_{\text{eff}}(z, z)$ corresponds to the dielectric permittivity of the relevant medium. In Fig. 4(b), this can be seen for the curves corresponding to $z = \{-1, 0, 1\}$. On the other hand, if the charge Q is located at the interface and the charge Q' approaches it infinitesimally close, they behave as in the two-layer system and, according to the discussion above, $\varepsilon_{\text{eff}} = \frac{1}{2}(\varepsilon_2 + \varepsilon_i)$, where i is the number of the corresponding cover. In Fig. 4(b), this can be seen for the curves corresponding to $z = \{-\frac{1}{2}, \frac{1}{2}\}$.

Then, there arises a question: How does the dependence $\varepsilon_{\text{eff}}(z, z')$ change when the charge Q crosses the interface? This issue was briefly and qualitatively discussed (the "double jump") in the previous subsection [Eqs. (17) and (18)]. To illustrate the answer, we performed calculations for the $\{z\}$ sets corresponding to the charge Q crossing the interfaces at $-\frac{1}{2}$ [Fig. 6(a)] and $\frac{1}{2}$ [Fig. 6(b)]. Again, the $w(z, z')$ dependencies (the upper subpanels) are not of much help in this regard. The singularities seem to be rather symmetric, and only their width changes depending on where the charge Q is located. Two lower subpanels provide more detailed information. However, they still leave uncertainties concerning the coordinate dependence of ε_{eff}.

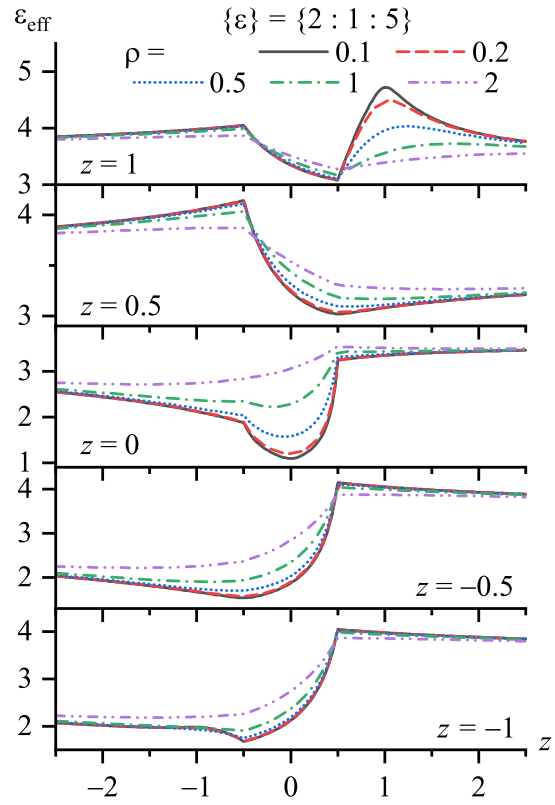

FIG. 5. The same as in Fig. 3(c), but for various ρ.

A definite answer to the question is given by Fig. 7, which corresponds to the lower panel of Fig. 6(a) describing the cases where the charge Q is extremely close to the $(-\frac{1}{2})$ interface. One can see that the corresponding $\varepsilon_{\text{eff}}(z, z')$ dependencies tend to something like a δ function as the charge

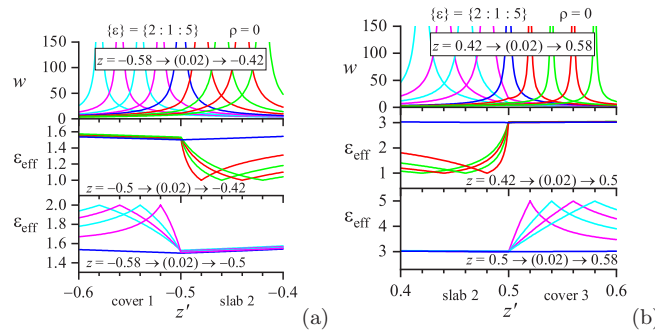

FIG. 6. Dependencies $w(z')$ and $\varepsilon_{\text{eff}}(z')$ for $\{\varepsilon\} = \{2 : 1 : 5\}$, $\rho = 0$, and various z near the $(-\frac{1}{2})$ (a) and $(\frac{1}{2})$ (b) interfaces.

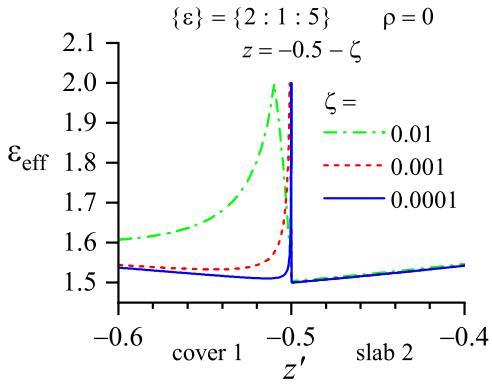

FIG. 7. The same as in the lower panel of Fig. 6(a), but for z extremely close to the $(-\frac{1}{2})$ interface.

overlap point approaches the interface and we really have a transition between the bulk- and interface-dominating regimes discussed above. Thus, the charge Q crossing any interface provokes an abrupt modification of the $\varepsilon_{\rm eff}(z, z')$ dependence if both charges are on the same normal to the interfaces.

The numerical results of Figs. 6 and 7 can be qualitatively explained by analytical formulas (23) and (26). Indeed, if the charge Q is located at any point in cover 1 except at $z = -\frac{1}{2}$, only the first term in Eq. (23) is singular at $z' \to z$. Since

$$\lim_{\alpha\to 0} \Phi\left(-\Lambda, 1, \frac{\alpha}{2}\right) \to \frac{2}{\alpha}, \tag{27}$$

we obtain that $\varepsilon_{\rm eff} \to \varepsilon_1 = 2$. It is exactly what we see in the lower panel of Fig. 6(a) to the left from $z' = -\frac{1}{2}$. At the same time, if $z = -\frac{1}{2}$, the fourth term in Eq. (23) also becomes singular at $z' \to z - 0$. In this case, the sum of two terms leads to

$$\varepsilon_{\rm eff} \to \left[\frac{1}{2\varepsilon_1}(2 - 2\lambda_{21})\right]^{-1} = \frac{\varepsilon_1 + \varepsilon_2}{2} = 1.5.$$

One can see a clear illustration of this fact in Fig. 7. If it were no other (at $z = \frac{1}{2}$) interface, this value would be retained for z' located to the right from $z = -\frac{1}{2}$, but the polarization charges at the $\frac{1}{2}$ interface violate this permanence.

Almost the same scenario takes place on the other side of the $-\frac{1}{2}$ interface [the middle panel in Fig. 6(a)]. If $z \neq -\frac{1}{2}$, only the first term in Eq. (25) is singular at $z' \to z$ so that, again according to limit (27), $\varepsilon_{\rm eff} \to \varepsilon_2 = 1$. If $z = -\frac{1}{2}$ and $z' \to z + 0$, then $\varepsilon_{\rm eff}$ is determined by the first and second terms in Eq. (25), and again

$$\varepsilon_{\rm eff} \to \left[\frac{1}{2\varepsilon_2}(2 + 2\lambda_{21})\right]^{-1} = \frac{\varepsilon_1 + \varepsilon_2}{2} = 1.5.$$

Thus, we obtain drastically different behavior of $\varepsilon_{\rm eff}$ depending on whether the charges are in the same layer or are separated by the interface. Those dependencies demonstrate a "double jump" as one of the charges crosses the interface. If this charge is located at the interface, we obtain a chevronlike $\varepsilon_{\rm eff}$ dependence owing to the influence of polarization charges emerging at the other interface [the $(z = -0.5)$ curve in the middle and lower panels of Fig. 6(a)].

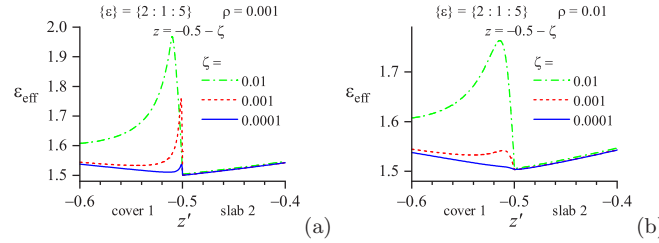

FIG. 8. The same as in Fig. 7, but for $\rho = 0.001$ (a) and 0.01 (b).

However, if the lateral distance between the charges is finite, $\rho \neq 0$, there is no double jump. This is illustrated in Fig. 8 for the lateral distances $\rho = 0.001$ [Fig. 8(a)] and 0.01 [Fig. 8(b)]. These figures are analogs of Fig. 7. Now, the trend $\varepsilon_{\rm eff}(z, z') \to \varepsilon_1$ when the charges maximally approach each other [see Eq. (17)] disappears. Instead, another limit (18) is realized and the $\varepsilon_{\rm eff}(z, z')$ dependencies evolve smoothly.

Figure 9 demonstrates the counterparts of Figs. 3(a) and 5 but for the "monotonous" set of the layer dielectric functions $\{\varepsilon\} = \{1 : 2 : 5\}$. The same, but for the set $\{\varepsilon\} = \{1 : 5 : 2\}$, is depicted in Fig. 10.

Long-range asymptotics

The results presented above confirm the common sense reasoning that the most interesting features in the interaction between charges in three-layer systems of classic insulators are observed if the distance between the charges is comparable with the interlayer width L and the charges are not located too far from the slab. Therefore, all illustrative dependencies were chosen on the basis of this consideration. On the other hand, in Sec. II A, it was shown that the interaction between the charges separated by large distances d has asymptotics (16). The word "large" means that this distance must considerably exceed the slab width (in the normalized notation, $d \gg 1$) irrespective of where the charges are located and how the segment connecting them is oriented with respect to the interfaces. So, it is of interest to determine how the indicated asymptotics is realized. For illustration, we took the charge Q to be at rest in one of the media (at $z = -1,\ 0$, or 1), whereas the charge Q' moves either in parallel to the interfaces (also

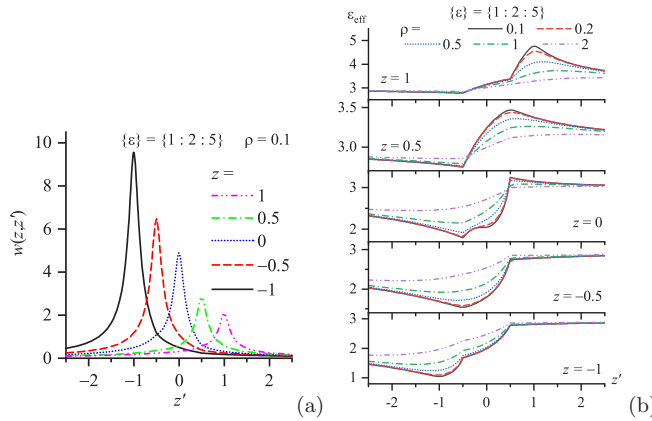

FIG. 9. The same as in Figs. 3(a) and 3(c), but for $\{\varepsilon\} = \{1 : 2 : 5\}$.

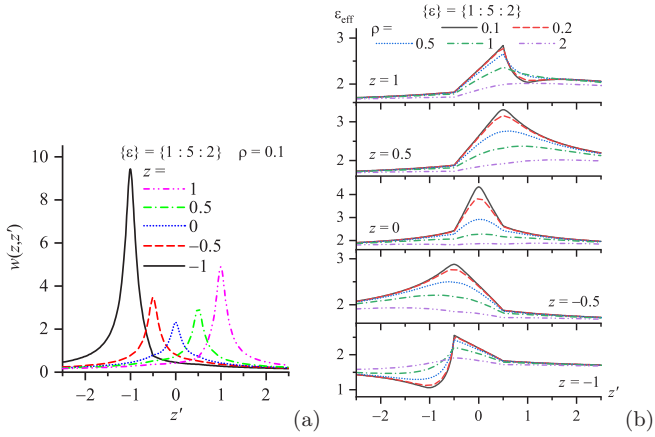

FIG. 10. The same as in Figs. 3(a) and 3(c), but for $\{\varepsilon\} = \{1 : 5 : 2\}$.

at $z' = -1,\ 0$, or 1) or perpendicularly to them at the lateral distance $\rho = 0,\ 1$, or 2 from the charge Q.

The corresponding calculation result for the $\{\varepsilon\}$ set $\{2 : 1 : 5\}$ is shown in Fig. 11. Here, the long-range asymptotic value is $\frac{1}{2}(\varepsilon_1 + \varepsilon_3) = 3.5$ and is indicated by thin dashed lines. Figure 11(a) corresponds to the "parallel" motion mode, and Fig. 11(b) to the "normal" one. The plotted dependencies confirm the theoretical result: if the intercharge distance is large enough, the charges cease to "feel" the slab, even if they are located in it, and the system becomes "effectively two layered," i.e., composed of semi-infinite media 1 and 3. However, this asymptotics can be reached at rather large distances between the charges.

Analogous results obtained for two other chosen $\{\varepsilon\}$ sets $\{1 : 2 : 5\}$ and $\{1 : 5 : 2\}$ are shown in Figs. 12 and 13, respectively.

C. Image-charge interpretation of the obtained formulas

It is possible and instructive to interpret the formulas obtained above for the interaction energy w_{ij} in the form of infinite series in a close analogy to the related problem of the image-charge interaction in three-layer structures [92], where the infinite series approach is quite traditional [85–90]. We recall that in the framework of the image-force theory, the potential created at some location by a point charge and concomitant polarization charges induced by it can be calculated in an equivalent and more simple way [85,127]. Namely, one

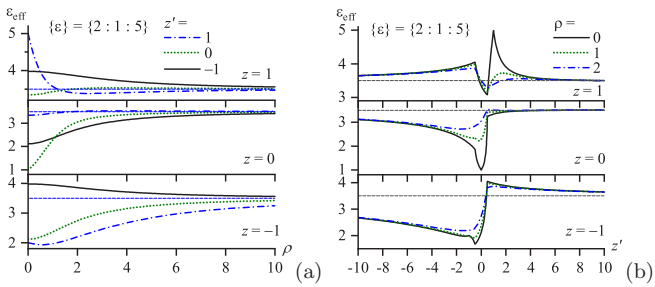

FIG. 11. Long-range $\varepsilon_{\text{eff}}(\rho, z' = \text{const})$ (a) and $\varepsilon_{\text{eff}}(z', \rho = \text{const})$ (b) dependencies for various z and $\{\varepsilon\} = \{2 : 1 : 5\}$.

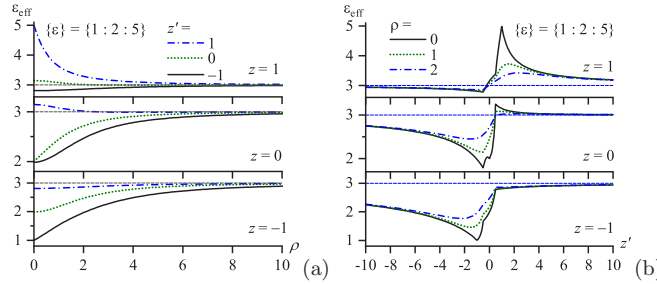

FIG. 12. The same as in Fig. 11, but for $\{\varepsilon\} = \{1 : 2 : 5\}$.

should sum up the Coulomb potential created by the given point charge in a fictitious infinite homogeneous medium with ε corresponding to the point of charge location and the potentials of the extended polarization charges. The latter potentials are equivalent to those of point image charges located in the same fictitious infinite homogeneous medium but at certain positions beyond the region concerned.

Similarly, in our case, we can consider any $w_{ij}(z, z')$ as (i) the interaction energy of the charge Q located at z with the charge Q' located at z' and its polarization charges located somewhere or (ii) the interaction energy of the charge Q' located at z' with the charge Q located at z and polarization charges induced by the latter; anyway, the lateral distance between them equals ρ. The analysis is convenient to be carried out on the basis of the template

$$\left\{\frac{1}{\varepsilon}\right\} \frac{\{\text{charge}\}_Q \times \{\text{charge}\}_{Q'}}{\sqrt{\rho^2 + (\{z\}_Q - \{z'\}_{Q'})^2}} \tag{28}$$

normalized according to Eq. (2). Each $\{\ldots\}_Q$ or $\{\ldots\}_{Q'}$ complex contains the relevant quantity for the corresponding (indicated as the subscript) charge and the common $\{\ldots\}$ prefactor is associated with the inverse dielectric permittivity of the fictitious infinite homogeneous medium.

As an example, let us consider Eq. (6).

(i) The charge Q (medium 3) is in the electrostatic field of the charge Q' (medium 2) and its polarization charges. Then, formula (6) should be rewritten in the form

$$\begin{aligned} w_{32} = &\sum_{i=0}^{\infty} \left\{\frac{1}{\varepsilon_3}\right\} \frac{\{1\}_Q \times \left\{\frac{\varepsilon_3}{(\varepsilon_2+\varepsilon_3)}(-\Lambda)^i\right\}_{Q'}}{\sqrt{\rho^2 + (\{z\}_Q - \{z' - 2i\}_{Q'})^2}} \\ &+ \sum_{i=0}^{\infty} \left\{\frac{1}{\varepsilon_3}\right\} \\ &\times \frac{\{1\}_Q \times \left\{-\frac{\varepsilon_3(\varepsilon_1-\varepsilon_2)}{(\varepsilon_1+\varepsilon_2)(\varepsilon_2+\varepsilon_3)}(-\Lambda)^i\right\}_{Q'}}{\sqrt{\rho^2 + (\{z\}_Q - \{-z' - 1 - 2i\}_{Q'})^2}}. \end{aligned} \tag{29}$$

We see that this is the interaction of the charge Q with two infinite sets of charges. One of them consists of the charges $\frac{\varepsilon_3(-\Lambda)^i}{(\varepsilon_2+\varepsilon_3)}Q'$ $(i = 0 \ldots \infty)$, each having the z coordinate equal to $z' - 2i$ and located at the lateral distance ρ (along the same normal to the interfaces) from the charge Q. The other set consists of the charges $-\frac{\varepsilon_3(\varepsilon_1-\varepsilon_2)(-\Lambda)^i}{(\varepsilon_1+\varepsilon_2)(\varepsilon_2+\varepsilon_3)}Q'$ $(i = 0 \ldots \infty)$, each

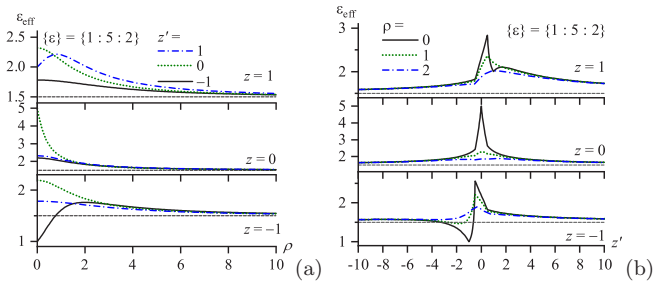

FIG. 13. The same as in Fig. 11, but for $\{\varepsilon\} = \{1 : 5 : 2\}$.

having the z coordinate equal to $-z' - 1 - 2i$ and located at the same lateral distance ρ (along the same normal to the interfaces as the previous charge set) from the charge Q. All charges are located in the infinite medium 3.

(ii) The charge Q' (medium 2) is in the electrostatic field of the charge Q (medium 3) and its polarization charges. Then, formula (6) should be rewritten in the form

$$w_{32} = \sum_{i=0}^{\infty} \left\{ \frac{1}{\varepsilon_2} \right\} \frac{\left\{ \frac{\varepsilon_2}{(\varepsilon_2+\varepsilon_3)} (-\Lambda)^i \right\}_Q \times \{1\}_{Q'}}{\sqrt{\rho^2 + (\{z'\}_{Q'} - \{z+2i\}_Q)^2}} + \sum_{i=0}^{\infty} \left\{ \frac{1}{\varepsilon_2} \right\} \times \frac{\left\{ -\frac{\varepsilon_2(\varepsilon_1-\varepsilon_2)}{(\varepsilon_1+\varepsilon_2)(\varepsilon_2+\varepsilon_3)} (-\Lambda)^i \right\}_Q \times \{1\}_{Q'}}{\sqrt{\rho^2 + (\{z'\}_{Q'} - \{-z-1-2i\}_Q)^2}}. \quad (30)$$

Quite similarly, we see that this is the interaction of the charge Q' with two infinite sets of charges arranged along the same normal to the interfaces at the lateral distance ρ from the charge Q'. The charges $\frac{\varepsilon_2(-\Lambda)^i}{(\varepsilon_2+\varepsilon_3)} Q$ $(i = 0 \ldots \infty)$ of one set have the z coordinates equal to $z + 2i$ and the charges $-\frac{\varepsilon_2(\varepsilon_1-\varepsilon_2)(-\Lambda)^i}{(\varepsilon_1+\varepsilon_2)(\varepsilon_2+\varepsilon_3)} Q$ $(i = 0 \ldots \infty)$ of the other set have the z coordinates equal to $-z - 1 - 2i$. Now, all charges are located in the infinite medium 2.

In the both cases, the sign of the charges in both sets will either alternate (if $\Lambda > 0$) or remain invariant (if $\Lambda < 0$).

But what if either of the charges is or both of them are located at the interfaces? We may be strictly governed by rule (4). But, we propose another solution, which can be useful in certain cases. In particular, in case (i), formula (29) can be rewritten in the form

$$w_{32} = \sum_{i=0}^{\infty} \left\{ \frac{(-\Lambda)^i}{(\varepsilon_2+\varepsilon_3)} \right\} \frac{\{1\}_Q \times \{1\}_{Q'}}{\sqrt{\rho^2 + (\{z\}_Q - \{z'-2i\}_{Q'})^2}} + \sum_{i=0}^{\infty} \left\{ -\frac{(\varepsilon_1-\varepsilon_2)(-\Lambda)^i}{(\varepsilon_1+\varepsilon_2)(\varepsilon_2+\varepsilon_3)} \right\} \times \frac{\{1\}_Q \times \{1\}_{Q'}}{\sqrt{\rho^2 + (\{z\}_Q - \{-z'-1-2i\}_{Q'})^2}}. \quad (31)$$

Formally, according to template (28), the first sum can be regarded as a linear combination of interaction between the charge Q and a set of identical(!) charges Q' through a set of channels $i = 0 \ldots \infty$. In each ith channel, the charges Q and Q' (now they are treated on equal footing) are arranged as described for the first set in case (i), but the effective dielectric constant of the ith fictitious infinite medium equals $\frac{\varepsilon_2+\varepsilon_3}{(-\Lambda)^i}$, i.e., it can even be negative. The second sum is interpreted analogously. The advantage of this approach consists in the formal equivalence of the charges and their images (all modifications are related to the properties of the medium in the corresponding interaction channel) and the independence of where the charges are located: in a certain medium or at the medium interface, which should facilitate further consideration of more complicated entities. Case (ii) can be treated similarly.

III. VERTICAL CHARGE-CHARGE INTERACTION ACROSS THE SLAB

As stems from Eqs. (20)–(25), when the charges are located on the same normal to the interfaces, the exact formulas for the charge-charge interaction can be expressed in terms of the Lerch transcendent Φ [128]. At the same time, the vertical arrangement of opposite-sign charges is the most likely one since they tend to approach each other as closely as possible, which is attained at $R = 0$. Therefore, the exact formulas are luckily able to represent the most important and abundant case of the interlayer electron-hole interaction. Equation (22) for the electron-hole attraction across the slab is the simplest one among Eqs. (20)–(25) and turns out to be the most significant for applications. Indeed, it describes, in particular, two experimental setups with the remote electron-hole attraction. We mean the formation of the strongly bound interlayer Wannier-Mott excitons [34–37,129], as well as superfluid electron-hole pairs spatially separated by the interlayer (especially, by the vacuum gap) [38–41,130–134]. Both scenarios can be realized in various layered van der Waals heterostructures [30,36,135–137], in particular, transition metal dichalcogenides [93,129,138,139], $A_{III}B_V$-based alternating layers [41,140–142], suspended non–van der Waals–type layered Bi_2O_2Se semiconductors [143], or hybrid perovskite semiconductors [25].

As a rule, the formation of excitons in the slabs of three-layer systems is considered in the framework of the Rytova-Keldysh approximation (RKA) [1,32]. A detailed analysis of the latter was done in our work [33]. The RKA expression for the energy of charge-charge interaction in the case of symmetric structures ($\varepsilon_1 = \varepsilon_3 = \varepsilon$) and for $\varepsilon_2 \gg \varepsilon$ looks like (here, the variables are non-normalized, see Fig. 1)

$$W_{\mathrm{RKA}} = QQ' \frac{\pi}{\varepsilon_2 L} \left[\mathbf{H}_0\left(\frac{2\varepsilon}{\varepsilon_2} \frac{R}{L} \right) - N_0\left(\frac{2\varepsilon}{\varepsilon_2} \frac{R}{L} \right) \right], \quad (32)$$

where $\mathbf{H}_0$ and N_0 are the Struve and Neumann functions of the zeroth order, respectively. Note that formula (32) does not include the Z coordinates of the charges. Its long-range ($R/L \to \infty$) asymptotics is identical to asymptotics (16). The RKA is very popular in relevant studies (see references in Ref. [33], as well as Refs. [37,144–148]). Although being derived for the conditions $\varepsilon \ll \varepsilon_2$, $R \gg L$, and $L \to 0$, it is sometimes overused when applying outside the indicated parameter region.

In particular, it concerns the short-range ($R \to 0$) asymptotics. Since W_{RKA} does not depend on Z and Z', it diverges logarithmically as $R \to 0$ irrespective of the charge locations in the slab. However, it is already intuitively clear [and it can be easily verified using Eq. (10)] that the true $W_{22}(Z, Z', R \to 0)$ dependence must be finite if $Z \neq Z'$ and must have an R^{-1} pole otherwise. Since the required dependence is absent, the latter is often assumed to be the classical Coulomb one for an infinite medium with the dielectric permittivity equal to that of the slab ε_2.

Formula (22) differs substantially from the expression

$$w_{31}^{C}(z_3, z_1) = \frac{1}{\varepsilon_2 |z_3 - z_1|}, \tag{33}$$

naively adopted to describe interaction across the slab. To solve various problems based on the knowledge of charge-charge interaction through the interlayer, it is necessary to estimate this difference quantitatively. In the cases we are interested in, namely, the analysis of the electron-hole interaction in semiconductor heterostructures, we may put $z_3 = \frac{1}{2}$ and $z_1 = -\frac{1}{2}$ (of course, such an approximation is unsatisfactory, e.g., for electrons suspended far over thin helium films [45,46]). Then,

$$w_{31}\left(\frac{1}{2}, -\frac{1}{2}\right) = \frac{2\varepsilon_2}{(\varepsilon_1 + \varepsilon_2)(\varepsilon_3 + \varepsilon_2)} \Phi\left(-\Lambda, 1, \frac{1}{2}\right), \tag{34}$$

whereas

$$w_{31}^{C}\left(\frac{1}{2}, -\frac{1}{2}\right) = \frac{1}{\varepsilon_2}. \tag{35}$$

In terms of the effective dielectric function (26), one has an analytical expression for a three-layered heterostructure,

$$\varepsilon_{\mathrm{eff}} = \frac{(\varepsilon_1 + \varepsilon_2)(\varepsilon_3 + \varepsilon_2)}{2\varepsilon_2 \Phi\left(-\Lambda, 1, \frac{1}{2}\right)}, \tag{36}$$

whereas in case (34),

$$\varepsilon_{\mathrm{eff}}^{C} \equiv \varepsilon_2. \tag{37}$$

Our goal is to calculate the dependencies of the ratio $M = \varepsilon_{\mathrm{eff}}/\varepsilon_2$ on two relevant parameters $\varepsilon_1/\varepsilon_2$ and $\varepsilon_3/\varepsilon_2$. This ratio directly indicates the modification of the effective Coulomb interaction as compared to the naive classical scenario. In the general case, one has

$$M = \frac{(\varepsilon_1/\varepsilon_2 + 1)(\varepsilon_3/\varepsilon_2 + 1)}{2\Phi\left(-\Lambda, 1, \frac{1}{2}\right)}, \tag{38}$$

with

$$\Lambda = -\frac{(\varepsilon_1/\varepsilon_2 - 1)}{(\varepsilon_1/\varepsilon_2 + 1)} \frac{(\varepsilon_3/\varepsilon_2 - 1)}{(\varepsilon_3/\varepsilon_2 + 1)}. \tag{39}$$

The Lerch function in the denominator of Eq. (38) reduces to the algebraic functions

$$\Phi\left(-\Lambda, 1, \frac{1}{2}\right) = \begin{cases} \dfrac{1}{\sqrt{-\Lambda}} \ln \left| \dfrac{1 + \sqrt{-\Lambda}}{1 - \sqrt{-\Lambda}} \right| & \text{if } \Lambda < 0, \\ \dfrac{2}{\sqrt{\Lambda}} \arctan \sqrt{\Lambda} & \text{if } \Lambda > 0. \end{cases} \tag{40}$$

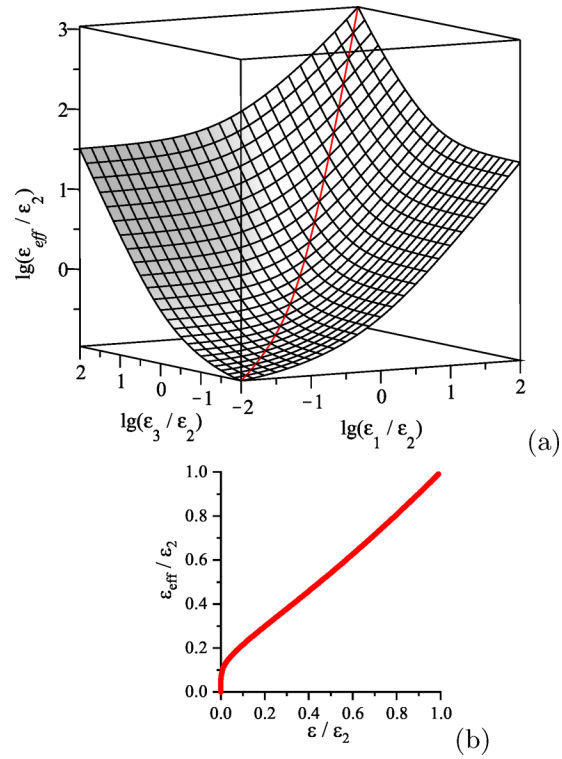

FIG. 14. (a) Dependence of the effective (normalized by ε_2) dielectric permittivity $\varepsilon_{\mathrm{eff}}$ of the slab [see Eq. (36)] for the interaction of the charges across the slab on the normalized dielectric permittivities of the covers (see further explanations in the text) in the log-log-log scale. The solid curve illustrates this dependence for the symmetric heterostructure ($\varepsilon_1 = \varepsilon_3 = \varepsilon$). This curve is also exhibited in (b) in the lin-lin scale.

In Fig. 14(a), the dependence $M(\varepsilon_1/\varepsilon_2, \varepsilon_3/\varepsilon_2)$ is shown in the log-log-log scale. It is clearly seen that M can be much larger or much less than unity, which means that the effective dielectric permittivity (36) can differ substantially from its slab counterpart ε_2.

For symmetric structures, when $\varepsilon_1 = \varepsilon_3 = \varepsilon$, the quantity M depends on only one parameter, $\mu = \varepsilon/\varepsilon_2$. This particular degenerate case is practically important, especially for sandwiches assumed to show the electron-hole superfluidity. Then, we have

$$\Lambda = -\frac{(\mu - 1)^2}{(\mu + 1)^2} < 0 \tag{41}$$

so that

$$\sqrt{-\Lambda} = \frac{|\mu - 1|}{(\mu + 1)} \tag{42}$$

and

$$M(\mu) = \frac{\mu^2 - 1}{2 \ln \mu} > 0. \tag{43}$$

If $\mu \gg 1$, which is realized, e.g., in the case of a vacuum gap between semiconductor layers, $M(\mu) \gg 1$. Therefore, in this situation, the layers strongly screen the electrostatic interaction, and the effective permittivity $\varepsilon_{\mathrm{eff}}$ is much larger than ε_2. The opposite case, when $\mu \ll 1$, describes, for instance,

the mutual interaction of charges located on the upper and lower boundaries of a semiconductor thin layer surrounded by the vacuum (or vapor media) [12,18,19,36,149–152]. Then, $M(\mu) \to 0$ abruptly [see Fig. 14(b) plotted in the lin-lin scale]. The dependence $M(\mu)$ is also shown in Fig. 14(a) as a thick line. Actually, a low effective dielectric permittivity can be achieved only when the suspended layer is made of ferroelectric [153–155].

The results shown in Fig. 14 can be directly checked when the calculated energy spectrum of interlayer excitons [34–37,129] is compared to the experimental data for various three-layer structures. The usage of the correct formula (36) and its particular cases can provide a satisfactory agreement with the experiment. One should bear in mind that the quantitative agreement can be achieved if one takes into account some additional factors, including the spatial dispersion of the dielectric permittivities.

To summarize this section, we emphasize that any oversimplified approach to the electrostatic phenomena in layered systems should be avoided. On the contrary, our approach is exact in the classical frame. Of course, to make more quantitative predictions for three-layer heterostructures, one must take into account the spatial dispersion of the dielectric permittivities in the framework of the same formal scheme [33,63,65].

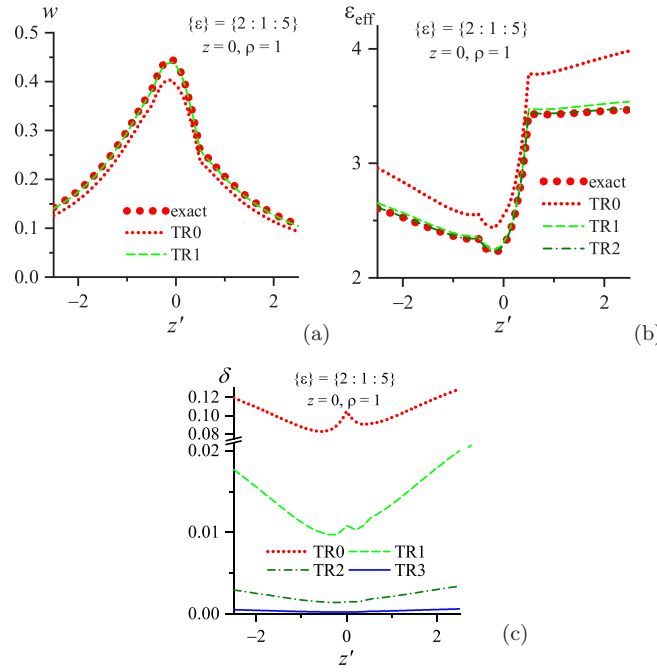

FIG. 15. Comparison of the exact dependencies $w(z')$ (a) and $\varepsilon_{\text{eff}}(z')$ (b) with their various TR approximations (see explanations and abbreviations in the text) for $\{\varepsilon\} = \{2 : 1 : 5\}$, $z = 0$, and $\rho = 1$. (c) The corresponding relative errors δ.

IV. APPROXIMATIONS

Modern computers allow numerical calculations to be performed at extremely high rates. However, very often we need to analytically estimate the behavior of a certain quantity, e.g., to analyze the dependence of its derivative on the problem parameters or use the result in further analytical calculations. Then, simple analytical approximations become highly desirable. This is true, in particular, for the electrostatic problem dealt with in this paper.

The formulas obtained for the w_{ij} branches in Sec. II A reduce this task to that of finding proper approximations for the function Ξ (see Appendix B). Series (B11) converge rather rapidly, which follows from inequality (B7) and the monotonically growing denominator of the series terms. Therefore, it is easy to find the calculation error if sum (B11) is truncated at its nth term:

$$\Xi_{\text{TR}n}(\Lambda, \rho, \alpha) = \sum_{i=0}^{n} \frac{(-\Lambda)^i}{\sqrt{\rho^2 + (\alpha + 2i)^2}}. \tag{44}$$

Such approximations will be referred to as TRn.

It is worth noting that the easiest way to calculate w and ε_{eff} quantities with a required accuracy is to follow the indicated routine. Just this method was used in the previous sections to calculate the $w(z, z', \rho)$ and $\varepsilon_{\text{eff}}(z, z', \rho)$ dependencies with a relative accuracy of 10^{-8}. As a result, the "exact" $w(z, z', \rho)$ values were calculated as the TR13 approximation for $\{\varepsilon\} = \{2 : 1 : 5\}$ with $\Lambda \approx -0.222$, as the TR10 approximation for $\{\varepsilon\} = \{1 : 2 : 5\}$ with $\Lambda \approx 0.143$, and as the TR15 approximation for $\{\varepsilon\} = \{1 : 5 : 2\}$ with $\Lambda \approx -0.286$ (the dielectric permittivities of the covers can be swapped). If we are interested in the w values with a "practical" accuracy of 10^{-2}, the application of the TR4, TR3, and TR4 approximations, respectively, are required.

Figure 15 demonstrates the application of various TR approximations to the $w(z, z')$ [Fig. 15(a)] and $\varepsilon_{\text{eff}}(z, z')$ [Fig. 15(b)] dependencies in the case when the charge Q is located at the center of the slab ($z = 0$) in the system with $\{\varepsilon\} = \{2 : 1 : 5\}$ and the charge Q' is shifted normally to the interfaces at the lateral distance $\rho = 1$. A comparison of the panels shows again that the $\varepsilon_{\text{eff}}(z, z')$ dependencies are more informative than the $w(z, z')$ ones. Figure 15(b) also testifies that the proposed approximations can well reproduce the local qualitative behavior of the dependencies. Since w and ε_{eff} are mutually reciprocal quantities [see Eq. (26)], the relative errors of their approximation are identical:

$$\delta(z, z') = \left| \frac{w^{\text{approx}}(z, z') - w(z, z')}{w(z, z')} \right| = \left| \frac{\varepsilon_{\text{eff}}^{\text{approx}}(z, z') - \varepsilon_{\text{eff}}(z, z')}{\varepsilon_{\text{eff}}(z, z')} \right|. \tag{45}$$

This quantity for the case concerned is depicted in Fig. 15(c). One can see that the TR0 approximation is rough even at low values of the parameter Λ so that higher-order approximations are required. This conclusion remains valid if the $w(z, z')$ dependencies are singular, which is illustrated in Fig. 16.

The growth of the absolute value of the parameter Λ enlarges the number of terms in sum (B11) to ensure a required accuracy. This fact is illustrated in Fig. 17 for a system with a moderate $|\Lambda| \approx 0.545$. An accuracy of 10^{-2} for w is reached only if an approximation not lower than TR8 is used. Moreover, we should take into account that each w_{ij} branch

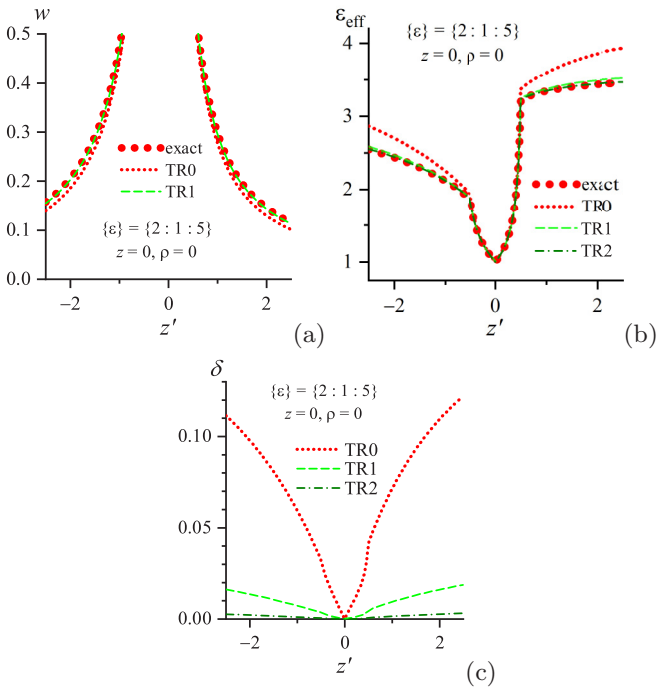

FIG. 16. The same as in Fig. 15, but for $\rho = 0$.

demands the calculation of several Ξ functions. So, it is more productive to consider integral (B5) itself.

It is very difficult, or even impossible, to substitute the Bessel function by something else in the whole integration range $q = [0, \infty)$ to produce a useful result. At the same time, the Bessel function itself gives a poor choice for other ways to calculate integral (B5) analytically. Our main idea was [33] to substitute the inverse denominator

$$\mathrm{Den}^{-1}(q) = \frac{1}{1 + \Lambda\, \exp(-2q)} \tag{46}$$

by a function with correct values at $q \to 0$ and $q \to \infty$, and with an "exponential" saturation at $q \to \infty$. The simplest variant is

$$\mathrm{Fun}(q) = 1 - \frac{\Lambda}{\Lambda + 1} \exp(-aq). \tag{47}$$

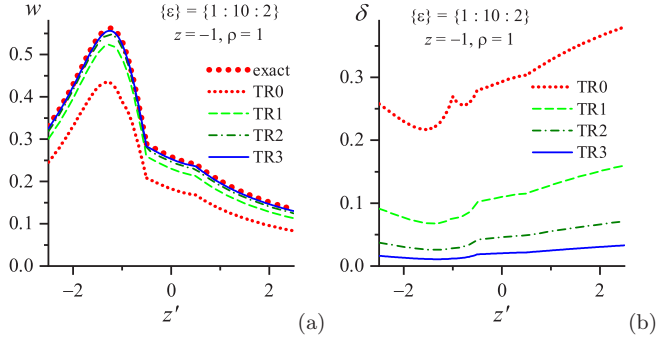

FIG. 17. The same as in Figs. 15(a) and 15(c), but for $\{\varepsilon\} = \{1 : 10 : 2\}$ and $z = -1$.

Then, the integral in Eq. (B5) can be calculated with the help of formula (B10):

$$\Xi(\Lambda, \alpha, \rho) \approx \frac{1}{\sqrt{\rho^2 + \alpha^2}} - \frac{\Lambda}{\Lambda + 1} \frac{1}{\sqrt{\rho^2 + (\alpha + a)^2}} \equiv \Xi_{\mathrm{EE}}(\Lambda, \alpha, \rho). \tag{48}$$

The "effective exponent" a remains to be found. The approximation was called "effective exponential" (EE).

For this purpose, earlier [33] we proposed the condition

$$\int_0^\infty \mathrm{Den}^{-1}(q)\, dq = \int_0^\infty \mathrm{Fun}(q)\, dq, \tag{49}$$

which brought about the value

$$a_{\mathrm{EE1}} = \frac{2\Lambda}{(1 + \Lambda)\ln(1 + \Lambda)}. \tag{50}$$

Another way to determine a is to demand that integral (B5) and its approximation (48) should have the same long-range (at $\alpha \to \infty$ and/or $\rho \to \infty$) asymptotics. The required value can be calculated by equating the dominant terms in the long-range asymptotics of expressions (B11) and (48). But attention should be paid to the fact that the factors $\exp(-\alpha q)$ (at $\alpha \to \infty$) and $J_0(\rho q)$ (at $\rho \to \infty$) in the integrand of Eq. (B5) make the behavior of the other factors insignificant at large q's: the former is a rapidly decaying function and the latter is a rapidly oscillating one. Only the integrand's behavior at $q \to 0$ matters in this case. The condition $\mathrm{Den}^{-1}(0) = \mathrm{Fun}(0)$ was already provided by selecting $\mathrm{Fun}(q)$ in form (47). Therefore, we put

$$\left[\frac{d}{dq}\mathrm{Den}^{-1}(q)\right]_{q=0} = \left[\frac{d}{dq}\mathrm{Fun}(q)\right]_{q=0}$$

and obtain

$$a_{\mathrm{EE2}} = \frac{2}{\Lambda + 1}. \tag{51}$$

The EE approximations $w_{\mathrm{EE}}(z, z')$ are described by formulas (5)–(10) and their modifications for $w(z, z')$ presented in Sec. II A, with the substitution of $\Xi_{\mathrm{EE}}(\Lambda, \alpha, \rho)$ [see notation (48)] instead of $\Xi(\Lambda, \alpha, \rho)$, and the relevant a_{EE} value [Eq. (50) or (51)].

In Fig. 18, the results of both approximations are shown for the $\{\varepsilon\}$ set $\{2 : 1 : 5\}$. Figure 18(a) corresponds to the lateral distance $\rho = 0.1$. The plots clearly demonstrate that the both approximations excellently reproduce the exact profiles of interaction energy, including cusps at the interfaces. The corresponding curves are almost indistinguishable from each other because the relative approximation errors within the indicated z' interval do not exceed 0.3% for the EE1 approximation and 0.6% for the EE2 one. At larger $|z'|$'s, the relative errors of both approximations decrease, with δ_{EE2} being two to three times lower than δ_{EE1}. This relationship between δ_{EE1} and δ_{EE2} at large $|z'|$'s also holds true for all parameter combinations illustrated below. The exhibited data testify that the proposed EE approximations retain the continuity of the $w_{\mathrm{EE}}(z, z')$ dependence if either or both charges cross any of the medium interfaces $z = \pm\frac{1}{2}$ provided that $\rho \neq 0$. This is a very useful property stemming from the continuity of the $w(z, z')$ dependence itself. Figure 18(b) corresponds to the

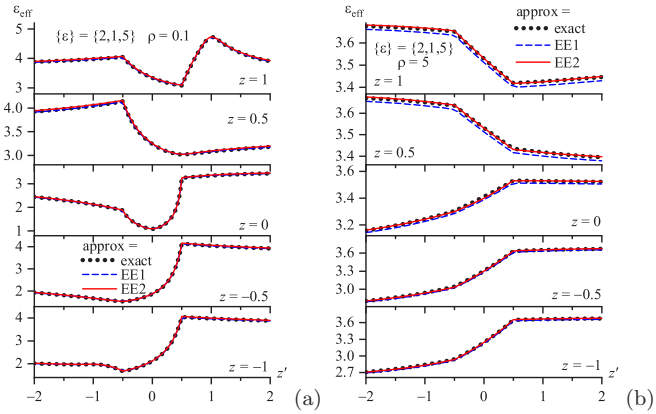

FIG. 18. Comparison of the exact $\varepsilon_{\text{eff}}(z')$ and their various EE approximations (see explanations and abbreviations in the text) for $\{\varepsilon\} = \{2:1:5\}$ and $\rho = 0.1$ (a) and 5 (b).

lateral distance $\rho = 5$. Here, the EE2 approximation is always better than the EE1 one: $\delta_{\text{EE1}} \lesssim 0.6\%$ and $\delta_{\text{EE2}} \lesssim 0.3\%$.

In Fig. 19, the same dependencies as in Fig. 18 are plotted but for the set $\{\varepsilon\} = \{1:5:2\}$, for which $|\Lambda|$ is larger (0.286 versus 0.222). In general, both approximations remain satisfactory but the relative errors increase: $\delta_{\text{EE1}} \lesssim 0.6\%$ and $\delta_{\text{EE2}} \lesssim 1\%$ at short distances [Fig. 19(a)], and $\delta_{\text{EE1}} \lesssim 0.9\%$ and $\delta_{\text{EE2}} \lesssim 0.3\%$ at long ones [Fig. 19(b)].

But, if we diminish $|\Lambda|$, the approximation quality becomes higher. In Fig. 20, the same dependencies are plotted for the dielectric constant set $\{\varepsilon\} = \{1:2:5\}$. Here, $\Lambda \approx 0.14$, which is the smallest value among the considered $\{\varepsilon\}$ sets. As a result, the quality of both approximations is also the best: $\delta_{\text{EE1}} \lesssim 0.1\%$ and $\delta_{\text{EE2}} \lesssim 0.16\%$ at short distances [Fig. 20(a)], and $\delta_{\text{EE1}} \lesssim 0.15\%$ and $\delta_{\text{EE2}} \lesssim 0.08\%$ at long ones [Fig. 20(b)].

Thus, the proposed EE approximations provide excellent results for the parameter sets considered above. The EE1 variant is better at short distances between the charges, and the EE2 variant has an advantage at long ones. Nevertheless, let us examine those approximations more attentively. A comparison of formulas (48) and (44) shows that, in essence, the former can be considered similar to the TR1 approximation: the zeroth-order term exactly reproduces the dominant term

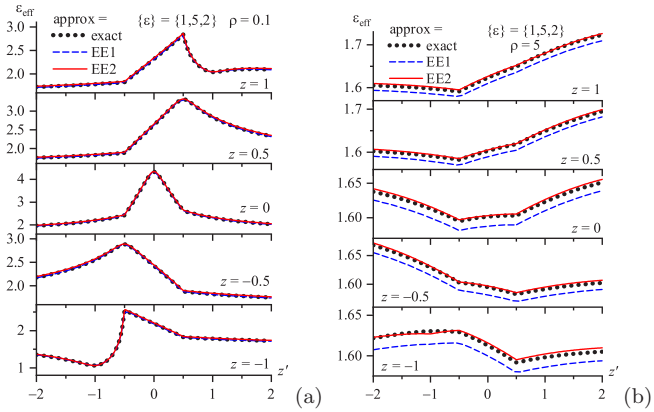

FIG. 19. The same as in Fig. 18, but for $\{\varepsilon\} = \{1:5:2\}$.

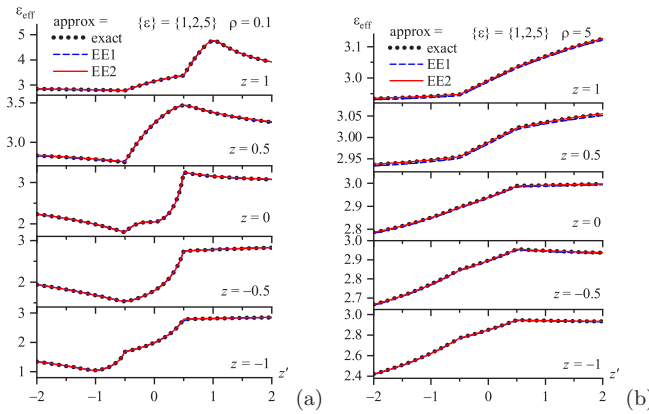

FIG. 20. The same as in Fig. 18, but for $\{\varepsilon\} = \{1:2:5\}$.

in series (B11), whereas the second one approximately substitutes the sum of all other terms. In both cases, the correction to the first (dominant) term is governed by the parameter Λ: the smaller the Λ magnitude, the better approximation. Therefore, it is of interest to compare the EE and TR approximations.

In Fig. 21, we did it for the toy system $\{\varepsilon\} = \{2:1:5\}$ in a wider interval of the parameter $z' = [-40, 40]$. The figure clearly demonstrates the following facts: (i) the EE1 approximation is better at short $|z - z'|$ spacings, and the EE2 approximation at long ones (recall that the EE2 approximation was designated to properly reproduce the long-range asymptotics); (ii) at short distances, the EE1 and EE2 approximations are comparable with the TR2 one; and (iii) the EE1 and EE2 approximations can be more successful than the higher-order TR approximations.

As stems from the results presented above, the quality of the EE approximation is better for smaller values of the parameter Λ. Nevertheless, the approximation EE remains adequate for rather large Λ's as well. In particular, in Fig. 22(a), which is a complement to Fig. 17(b), one can see that the EE1 approximation (we consider short distances) is at least

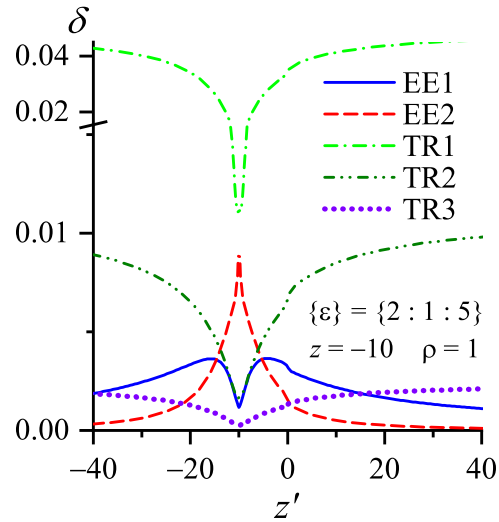

FIG. 21. Comparison of the relative errors δ given by all proposed approximations at short and large distances in the case $\{\varepsilon\} = \{2:1:5\}$, $z = -10$, and $\rho = 1$.

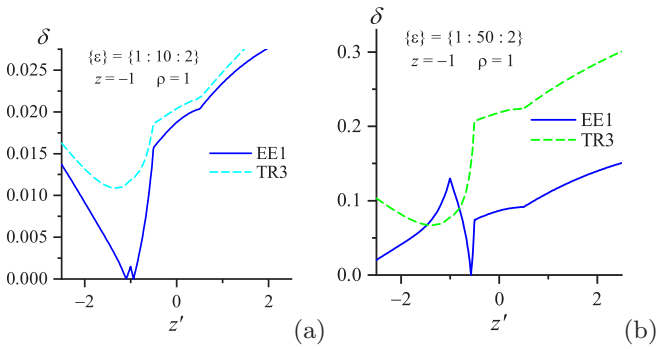

FIG. 22. Comparison of the TR3 and EE1 approximations in the case of large Λ values: $|\Lambda| \approx 0.545$ (a) and 0.887 (b).

not worse than the TR3 approximation at the moderate $|\Lambda| \approx 0.545$. But even at high $|\Lambda|$ magnitudes, the EE1 approximation provides reasonable estimations (to an accuracy of 10%–15%) for the $w(z, z')$ dependence, being much better than the TR3 [this is illustrated in Fig. 22(b) for the $\{\varepsilon\} = \{1 : 50 : 2\}$ heterostructure with $|\Lambda| \approx 0.887$].

Thus, the proposed approximations are a convenient tool for calculating the interaction energy of two charges in three-layer structures with a fairly high accuracy making use of simple analytical expressions. Nevertheless, they possess a shortcoming. Specifically, any proposed approximation of the interference terms induced by polarization charges at the interfaces (those are the terms containing the coefficient Λ) in the formulas for the w_{ii} branches [in particular, Eqs. (5) and (10)] possesses a cusp at $z = z'$. Since the terms are proportional to Λ, the cusp is also comparatively small for small Λ's. This cusp can be almost unobservable against a steep background, as one can see from Fig. 17(a). Nevertheless, Fig. 17(b) clearly demonstrates that this unphysical cusp does exist, being especially pronounced for the TR0 approximation.

However, the situation may change if $|\Lambda|$ is large enough and the background is not steep. Figure 23 demonstrates the calculated $w(z = -1, z')$ dependencies for a system with

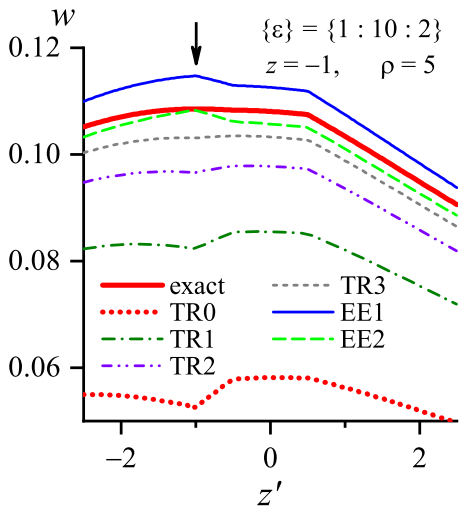

FIG. 23. Possible manifestation of unphysical extrema in the w approximation dependencies (see explanations in the text).

$\{\varepsilon\} = \{1 : 10 : 2\}$ (the same as in Fig. 17) but for the lateral intercharge distance $\rho = 5$. At their nearest approach, the charges are located rather far from each other, and the maximum of the exact $w(z = -1, z')$ dependence (the thick curve) is wide and smooth. It makes it easy to observe cusps arising in the approximation curves when the charge Q' crosses the z level of the charge Q ($z = z' = 1$, indicated by an arrow). As a result, there appears an unphysical minimum or maximum in the corresponding dependence. The figure testifies that the indicated cusp is effectively smoothed out as the order of TR approximation grows. But, the cusps in the proposed two EE approximations are uncontrollable for the given problem parameters.

Whether this cusp matters or not depends on the problem concerned. For instance, the charge interaction energy is only one component of the total electrostatic energy of charges in the heterostructure. To obtain the total energy, the interaction energy has to be combined with the image force energy [the self-energies of both charges, see Eq. (1)] [92], which can obscure the unphysical behavior of $w(z, z')$. Anyway, it is not possible now to give general recommendations how to exterminate those tiny false features.

This minor difficulty is, however, practically insignificant, whereas the approximations EE1 and EE2 *per se* may be useful as an analytical guide to the problems dealing with the electrostatic energy of charges in layered systems, being a preliminary step before carrying out cumbersome numerical calculations.

V. CONCLUSIONS

In this paper, a theoretical framework capable of studying the charge-charge interaction in three-layer heterostructures with different dielectric permittivities of the constituent media has been outlined. The specific calculations were carried out in the classical electrostatic approximation, when all dielectric permittivities are constants. Compact formulas were obtained for all possible arrangements of charges. The results are expressed in terms of tabulated special functions when charges are positioned on the same normal to the layers. We demonstrated that the interaction energy dependencies on the charge-charge distances differ substantially from the Coulomb law. Therefore, we introduced the effective dielectric function ε_{eff} making the results concise and illustrative. The modification of the Coulomb law obtained here should be applied when studying various problems of the condensed matter physics. The necessity of the adequate treatment of the three-layer electrostatics is especially clear for electron-hole interaction leading to the formation of interlayer excitons and appearance of the excitonic lateral superfluidity.

ACKNOWLEDGMENTS

This research was performed in the framework of the Joint Ukrainian-Polish program (2022–2024), Grant No. 23. A.M.G. and A.I.V. were also supported by Grant No. 1.4.B-197 of the Institute of Physics of the National Academy of Sciences of Ukraine and M.S.L. was supported by Grant No. 2019/35/B/ST4/02086 of the Narodowe Centrum Nauki in Poland.

APPENDIX A

Let us consider a system consisting of three plane-parallel layers and invariant with respect to translations along the layer interfaces. Each ith layer is a medium described by the dielectric function $\varepsilon_i(\mathbf{k}, \omega)$, $i = 1, 2, 3$. Two point charges Q and Q' are located in this system at the coordinates Z and Z', respectively (reckoned perpendicularly to the interfaces). They are separated by the lateral (along the interfaces) distance R (see Fig. 1). Then, their electrostatic interaction energy W can be written in the form [33,63,65]

$$W(Z, Z', R) = -2QQ' \int_0^\infty K\, dK\, D(K, Z, Z') J_0(KR), \quad \text{(A1)}$$

where J_0 is the zeroth-order Bessel function of the first kind and D is Green's function of the problem.

In the system concerned, a slab ($i = 2$) of thickness L is confined between two semi-infinite covers ($i = 1, 3$), so that we have a good natural scaling length parameter L. It is convenient to perform the corresponding normalization for all relevant quantities in the integrand of formula (A1),

$$q = KL, \quad z^{(\prime)} = Z^{(\prime)}/L, \quad \rho = R/L, \quad \text{(A2)}$$

and the interaction energy itself,

$$w(z, z', \rho) = \left(\frac{QQ'}{L}\right)^{-1} W = -2\int_0^\infty q\, dq\, D(q, z, z') J_0(q\rho). \quad \text{(A3)}$$

The kernel $D(q, z, z')$ is rather cumbersome. Its form strongly depends on the media where the charges are positioned [see Eq. (4)]. Nevertheless, the expression for $D(q, z, z')$ can be simplified by introducing the following quantities generalizing (for $z \neq 0$) the so-called inverse surface dielectric functions [57,58,156]

$$a_{1,3}(q, z) = \frac{1}{\pi} \int_{-\infty}^{\infty} \frac{dk_\perp \cos k_\perp z}{(k_\perp^2 + q^2)\varepsilon_{1,3}(\mathbf{q}, k_\perp, \omega)} \quad \text{(A4)}$$

and

$$a_{S,A}(q, z) = 2 \sum_{k_\perp^{S,A}} \frac{\exp\left[ik_\perp\left(z + \frac{1}{2}\right)\right]}{(k_\perp^2 + q^2)\varepsilon_2(\mathbf{q}, k_\perp, \omega)}, \quad \text{(A5)}$$

where

$$k_\perp^S = 2n\pi, \quad k_\perp^A = (2n+1)\pi, \quad n = 0, \pm 1, \pm 2, \ldots .$$

Then, the kernel $D(q, z, z')$ looks like

$$D = \frac{A(q, z)B(q, z') + \tilde{A}(q, z)\tilde{B}(q, z')}{C(q)} - F(q, z, z'), \quad \text{(A6)}$$

where (to shorten the formulas, we omit the q dependence from the argument list for a_i)

$$A(q, z) = \begin{cases} a_1(z + \frac{1}{2}) & \text{if med}(z) = 1, \\ -a_S(z) & \text{if med}(z) = 2, \\ a_3(z - \frac{1}{2}) & \text{if med}(z) = 3; \end{cases} \quad \text{(A7)}$$

$$\tilde{A}(q, z) = \begin{cases} a_1(z + \frac{1}{2}) & \text{if med}(z) = 1, \\ -a_A(z) & \text{if med}(z) = 2, \\ -a_3(z - \frac{1}{2}) & \text{if med}(z) = 3; \end{cases} \quad \text{(A8)}$$

$$B(q, z') = \begin{cases} a_1(z' + \frac{1}{2})[a_A^* + a_3^*] & \text{if med}(z) = 1, \\ -\frac{1}{2}[a_S(z') + a_A(z')][a_A^* + a_3^*] - \frac{1}{2}[a_S(z') - a_A(z')][a_A^* + a_1^*] & \text{if med}(z) = 2, \\ a_3(z' - \frac{1}{2})[a_A^* + a_1^*] & \text{if med}(z) = 3; \end{cases} \quad \text{(A9)}$$

$$\tilde{B}(q, z') = \begin{cases} a_1(z' + \frac{1}{2})[a_S^* + a_3^*] & \text{if med}(z) = 1, \\ -\frac{1}{2}[a_S(z') + a_A(z')][a_S^* + a_3^*] + \frac{1}{2}[a_S(z') - a_A(z')][a_S^* + a_1^*] & \text{if med}(z) = 2, \\ -a_3(z' - \frac{1}{2})[a_S^* + a_1^*] & \text{if med}(z) = 3; \end{cases} \quad \text{(A10)}$$

$$C(q) = [a_S^* + a_1^*][a_A^* + a_3^*] + [a_S^* + a_3^*][a_A^* + a_1^*]; \quad \text{(A11)}$$

$$F(q, z, z') = \begin{cases} \frac{1}{2}\left[a_1\left(\left|z + \frac{1}{2}\right| + \left|z' + \frac{1}{2}\right|\right) + a_1\left(\left|z + \frac{1}{2}\right| - \left|z' + \frac{1}{2}\right|\right)\right] & \text{if med}(z) = \text{med}(z') = 1, \\ \frac{1}{4}\left[a_S(z + z' + \frac{1}{2}) + a_S(z - z' - \frac{1}{2})\right] & \\ \quad + \frac{1}{4}\left[a_A(z + z' + \frac{1}{2}) + a_A(z - z' - \frac{1}{2})\right] & \text{if med}(z) = \text{med}(z') = 2, \\ \frac{1}{2}\left[a_3\left(\left|z - \frac{1}{2}\right| + \left|z' - \frac{1}{2}\right|\right) + a_3\left(\left|z - \frac{1}{2}\right| + \left|z' - \frac{1}{2}\right|\right)\right] & \text{if med}(z) = \text{med}(z') = 3, \\ 0 & \text{otherwise}; \end{cases} \quad \text{(A12)}$$

and

$$a_1^* = a_1(0), \quad a_3^* = a_3(0), \quad a_S^* = a_S\left(-\tfrac{1}{2}\right), \quad a_A^* = a_A\left(-\tfrac{1}{2}\right). \quad \text{(A13)}$$

Note that the presented formulas can also be used to calculate the image force energy $W_{\text{im}}(Z)$, i.e., the energy of interaction between the charge Q located at the point with the coordinate Z (the coordinates X and Y can be arbitrary) and the self-induced polarization charges at both interfaces. Namely,

$$W_{\text{im}}(Z) = \frac{1}{2} \lim_{\substack{Z' \to Z \\ R \to 0 \\ Q' \to Q}} \left[W(Z, Z, R) - \frac{QQ'}{\varepsilon |Z - Z'|} \right]. \quad \text{(A14)}$$

Here, ε is the dielectric constant of the medium where the charge is located, the last term in the brackets is the bulk self-energy of the examined charge (infinite at $Z = Z'$) [157], and the multiplier $\frac{1}{2}$ takes into account the fact that the polarization charges are not external ones and appear only under the influence of the charge Q. The insertion of this multiplier

can be justified, e.g., by the Güntelberg charging process [158–163]. It should be emphasized that in order to obtain the total energy of external charges in the polarized three-layer system, one should add terms $W(Z, Z', R)$ given by Eq. (A1), $W_{\rm im}(Z)$ given by Eq. (A14) and its counterpart $W_{\rm im}(Z')$ [see Eq. (1)]. This fact was recognized decades ago [87,91,164–166]. However, the correct analytical expressions for $W_{\rm im}(Z)$ in three-layered systems, which are expressed via the Lerch transcendent function [128] in the classical electrostatic framework, have been obtained only recently [92].

APPENDIX B

In the case of homogeneous nondispersive insulators ($\varepsilon_i = \text{const}$, $i = 1, 2, 3$), the functions $a_{1,3}(q, z)$ and $a_{S,A}(q, z)$ can be expressed analytically. In particular [128, Eq. (3.723.2)],

$$a_{1,3}(q, z) = \frac{1}{\varepsilon_{1,3} q} \exp(-q|z|). \tag{B1}$$

Formula (A5) can be rewritten in the form

$$a_{S,A}(q, z) = \frac{2}{\varepsilon_2} \sum_{k_\perp^{S,A}} \frac{\cos\left[k_\perp\left(z + \frac{1}{2}\right)\right]}{k_\perp^2 + q^2}. \tag{B2}$$

For calculations, let us apply the tabulated sum [128, Eq. (1.445.2)]

$$S_0(x, \alpha) = \sum_{k=1}^{\infty} \frac{\cos(kx)}{k^2 + \alpha^2} = \frac{\pi}{2\alpha} \frac{\cosh\alpha(\pi - x)}{\sinh\alpha\pi} - \frac{1}{2\alpha^2}$$

for $0 \leqslant x \leqslant 2\pi$.

Then,

$$\begin{aligned} S(n, x, \alpha) &= \sum_{k=-\infty}^{\infty} \frac{\cos(n\pi kx)}{(n\pi k)^2 + \alpha^2} \\ &= \frac{1}{(n\pi)^2} \left(\sum_{k=-\infty}^{-1} + \sum_{k=0} + \sum_{k=1}^{\infty} \right) \frac{\cos(k \cdot n\pi x)}{k^2 + \left(\frac{\alpha}{n\pi}\right)^2} \\ &= \frac{1}{\alpha^2} + \frac{2}{(n\pi)^2} S_0\left(n\pi x, \frac{\alpha}{n\pi}\right) \\ &= \frac{1}{n\alpha} \frac{\cosh\frac{(nx-1)\alpha}{n}}{\sinh\frac{\alpha}{n}}. \end{aligned}$$

Now,

$$S_{\rm even}(x, \alpha) = S(2, x, \alpha) = \frac{\cosh\left[\left(\frac{1}{2} - x\right)\alpha\right]}{2\alpha \sinh\frac{\alpha}{2}}$$

and

$$\begin{aligned} a_S(q, z) &= \frac{2}{\varepsilon_2} S_{\rm even}(z + \tfrac{1}{2}, q) \\ &= \begin{cases} \dfrac{1}{q\varepsilon_2} \dfrac{\cosh(qz)}{\sinh\left(\frac{q}{2}\right)} & \text{if } -\frac{1}{2} \leqslant z \leqslant \frac{1}{2}, \\ a_S(q, z \pm 1) & \text{otherwise.} \end{cases} \end{aligned} \tag{B3}$$

At the same time,

$$S_{\rm odd}(x, \alpha) = S(1, x, \alpha) - S_{\rm even}(x, \alpha) = \frac{\sinh\left[\left(\frac{1}{2} - x\right)\alpha\right]}{2\alpha \cosh\frac{\alpha}{2}}$$

and

$$\begin{aligned} a_A(q, z) &= \frac{2}{\varepsilon_2} S_{\rm odd}(z + \tfrac{1}{2}, q) \\ &= \begin{cases} -\dfrac{1}{q\varepsilon_2} \dfrac{\sinh(qz)}{\cosh\left(\frac{q}{2}\right)} & \text{if } -\frac{1}{2} \leqslant z \leqslant \frac{1}{2}, \\ -a_A(q, z \pm 1) & \text{otherwise.} \end{cases} \end{aligned} \tag{B4}$$

Then, the kernel $D(q, z, z')$ [see Eq. (A6)] transforms into a linear, specific for each $(\text{med}(z), \text{med}(z'))$ pair [see Eq. (4)], combination of integrals

$$\Xi(\Lambda, \alpha, \rho) = \int_0^\infty \frac{\exp(-\alpha q)}{1 + \Lambda \exp(-2q)} J_0(\rho q) dq, \tag{B5}$$

where $\alpha \geqslant 0$ and the parameter

$$\Lambda = \frac{(\varepsilon_1 - \varepsilon_2)(\varepsilon_2 - \varepsilon_3)}{(\varepsilon_1 + \varepsilon_2)(\varepsilon_2 + \varepsilon_3)} \tag{B6}$$

is less than unity by magnitude in almost all practically significant cases,

$$|\Lambda| < 1. \tag{B7}$$

One can see that $\Lambda \to 1$ in the cases $\varepsilon_1 \ll \varepsilon_2 \ll \varepsilon_3$ and $\varepsilon_1 \gg \varepsilon_2 \gg \varepsilon_3$. The limiting value $\Lambda = -1$ is realized if ε_2 is finite and $(\varepsilon_1, \varepsilon_3) \to \infty$ or if $\varepsilon_2 \to \infty$ and ε_1 and ε_3 are finite. It is convenient to express the parameter Λ as the product

$$\Lambda = \lambda_{12}\lambda_{23}, \tag{B8}$$

where

$$\lambda_{ij} = \frac{\varepsilon_i - \varepsilon_j}{\varepsilon_i + \varepsilon_j} \tag{B9}$$

in the case of two-layer system, i.e., if $\varepsilon_1 = \varepsilon_2$ or $\varepsilon_2 = \varepsilon_3$, the parameter Λ and either the parameter λ_{12} or λ_{23} equal zero.

Integral (B5) is not classified as a special function. Nevertheless, using the property (B7), we may expand the integrand in Eq. (B5) in a power series in Λ and then use the formula [128, Eq. (6.611.1)]

$$\int_0^\infty \exp(-\beta q) J_0(\rho q) dq = \frac{1}{\sqrt{\rho^2 + \beta^2}}, \tag{B10}$$

where $\beta \geqslant 0$. Then integral (B5) can be written in the form

$$\Xi(\Lambda, \rho, \alpha) = \sum_{i=0}^{\infty} \frac{(-\Lambda)^i}{\sqrt{\rho^2 + (\alpha + 2i)^2}}. \tag{B11}$$

By extracting the first summand in the sum, this formula can be rewritten as follows:

$$\Xi(\Lambda, \rho, \alpha) = \frac{1}{\sqrt{\rho^2 + \alpha^2}} - \Lambda\, \Xi(\Lambda, \rho, \alpha + 2), \tag{B12}$$

which allows the approximation of the next order of smallness in the parameter Λ to be obtained for the function $\Xi(\Lambda, \rho, \alpha)$. The inverse formula is also useful:

$$\Xi(\Lambda, \rho, \alpha) = \frac{1}{\Lambda\sqrt{\rho^2 + (\alpha - 2)^2}} - \frac{1}{\Lambda}\,\Xi(\Lambda, \rho, \alpha - 2). \tag{B13}$$

In the particular case $\rho = 0$,

$$\Xi(\Lambda, 0, \alpha) = \int_0^\infty \frac{\exp(-\alpha q)}{1 + \Lambda\exp(-2q)}dq = \sum_{i=0}^{\infty}\frac{(-\Lambda)^i}{\alpha + 2i} = \frac{1}{2}\Phi\Big(-\Lambda, 1, \frac{\alpha}{2}\Big), \tag{B14}$$

where Φ is the Lerch transcendent [128, section 9.55].

[1] L. V. Keldysh, Pis'ma Zh. Éksp. Teor. Fiz. **29**, 716 (1979) [JETP Lett. **29**, 658 (1979)].
[2] J. Katriel, Phys. Lett. A **101**, 158 (1984).
[3] V. M. Fomin and E. P. Pokatilov, Phys. Status Solidi B **129**, 203 (1985).
[4] E. P. Pokatilov, S. I. Beril, V. M. Fomin, and G. A. Pogorilko, Phys. Status Solidi B **130**, 619 (1985).
[5] E. P. Pokatilov, S. I. Beril, V. M. Fomin, and V. V. Kalinovskii, Phys. Status Solidi B **161**, 603 (1990).
[6] L. Wendler and B. Hartwig, J. Phys.: Condens. Matter **3**, 9907 (1991).
[7] X. Hong, T. Ishihara, and A. V. Nurmikko, Phys. Rev. B **45**, 6961 (1992).
[8] H. Mathieu, P. Lefebvre, and P. Christol, Phys. Rev. B **46**, 4092 (1992).
[9] A. Chernikov, T. C. Berkelbach, H. M. Hill, A. Rigosi, Y. Li, O. B. Aslan, D. R. Reichman, M. S. Hybertsen, and T. F. Heinz, Phys. Rev. Lett. **113**, 076802 (2014).
[10] S. Latini, T. Olsen, and K. S. Thygesen, Phys. Rev. B **92**, 245123 (2015).
[11] T. C. Berkelbach and D. R. Reichman, Annu. Rev. Condens. Matter Phys. **9**, 379 (2018).
[12] M. V. Durnev and M. M. Glazov, Usp. Fiz. Nauk **188**, 913 (2018).
[13] J.-Z. Zhang and J.-Z. Ma, J. Phys.: Condens. Matter **31**, 105702 (2019).
[14] B. Scharf, D. V. Tuan, I. Žutić, and H. Dery, J. Phys.: Condens. Matter **31**, 203001 (2019).
[15] A. Raja, L. Waldecker, J. Zipfel, Y. Cho, S. Brem, J. D. Ziegler, M. Kulig, T. Taniguchi, K. Watanabe, E. Malic, T. F. Heinz, T. C. Berkelbach, and A. Chernikov, Nat. Nanotechnol. **14**, 832 (2019).
[16] F. García-Flórez, L. D. A. Siebbeles, and H. T. C. Stoof, Phys. Rev. B **102**, 125303 (2020).
[17] L. V. Kulik, V. D. Kulakovskii, M. Bayer, A. Forchel, N. A. Gippius, and S. G. Tikhodeev, Phys. Rev. B **54**, R2335 (1996).
[18] Q. H. Wang, K. Kalantar-Zadeh, A. Kis, J. N. Coleman, and M. S. Strano, Nat. Nanotechnol. **7**, 699 (2012).
[19] A. V. Stier, N. P. Wilson, G. Clark, X. Xu, and S. A. Crooker, Nano Lett. **16**, 7054 (2016).
[20] A. V. Stier, N. P. Wilson, K. A. Velizhanin, J. Kono, X. Xu, and S. A. Crooker, Phys. Rev. Lett. **120**, 057405 (2018).
[21] G. Wang, A. Chernikov, M. M. Glazov, T. F. Heinz, X. Marie, T. Amand, and B. Urbaszek, Rev. Mod. Phys. **90**, 021001 (2018).
[22] I. Filikhin, R. Y. Kezerashvili, Sh. M. Tsiklauri, and B. Vlahovic, Nanotechnology **29**, 124002 (2018).
[23] D. B. Straus and C. R. Kagan, J. Phys. Chem. Lett. **9**, 1434 (2018).
[24] O. Ávalos Ovando, D. Mastrogiuseppe, and S. E. Ulloa, J. Phys.: Condens. Matter **31**, 213001 (2019).
[25] C. Katan, N. Mercier, and J. Even, Chem. Rev. **119**, 3140 (2019).
[26] Y. Xu, S. Liu, D. A. Rhodes, K. Watanabe, T. Taniguchi, J. Hone, V. Elser, and K. F. M. J. Shan, Nature (London) **587**, 214 (2020).
[27] S. T. Chui, N. Wang, and B. Tanatar, Phys. Rev. B **104**, 195432 (2021).
[28] E. Canel, M. P. Matthews, and R. K. P. Zia, Phys. Kondens. Materie **15**, 191 (1972).
[29] P. Cudazzo, I. V. Tokatly, and A. Rubio, Phys. Rev. B **84**, 085406 (2011).
[30] K. S. Thygesen, 2D Mater. **4**, 022004 (2017).
[31] D. Felbacq and E. Rousseau, Ann. Phys. **531**, 1800486 (2019).
[32] N. S. Rytova, Vestn. Mosk. Univ. **3**, 30 (1967) [arXiv:1806.00976 [cond-mat.mes-hall]].
[33] A. M. Gabovich and A. I. Voitenko, Condens. Matter **4**, 44 (2019).
[34] P. Rivera, J. R. Schaibley, A. M. Jones, J. S. Ross, S. Wu, G. Aivazian, P. Klement, K. Seyler, G. Clark, N. J. Ghimire, J. Yan, D. G. Mandrus, W. Yao, and X. Xu, Nat. Commun. **6**, 6242 (2015).
[35] H. Heo, J. H. Sung, S. Cha, B.-G. Jang, J.-Y. Kim, G. Jin, D. Lee, J.-H. Ahn, M.-J. Lee, J. H. Shim, H. Choi, and M.-H. Jo, Nat. Commun. **6**, 7372 (2015).
[36] N. P. Wilson, W. Yao, J. Shan, and X. Xu, Nature (London) **599**, 383 (2021).
[37] M. F. C. Martins Quintela, J. C. G. Henriques, and N. M. R. Peres, Phys. Rev. B **104**, 205433 (2021).
[38] S. I. Shevchenko, Fiz. Nizk. Temp. **2**, 505 (1976) [Sov. J. Low Temp. Phys. (Engl. Transl.) **2**, 1976 (1976)]
[39] Yu. E. Lozovik and V. I. Yudson, Zh. Éksp. Teor. Fiz. **71**, 738 (1976) [Sov. Phys. JETP **44**, 389 (1976)].
[40] D. V. Fil and S. I. Shevchenko, Fiz. Nizk. Temp. **44**, 1111 (2018) [Low Temp. Phys. **44**, 867 (2018)].
[41] S. Saberi-Pouya, S. Conti, A. Perali, A. F. Croxall, A. R. Hamilton, F. M. Peeters, and D. Neilson, Phys. Rev. B **101**, 140501(R) (2020).
[42] D. V. Fil and S. I. Shevchenko, Phys. Rev. B **103**, 205419 (2021).
[43] E. A. Eliseev, S. V. Kalinin, S. Jesse, S. L. Bravina, and A. N. Morozovska, J. Appl. Phys. **102**, 014109 (2007).
[44] M. Yelisieiev, P. Maksymovych, and A. N. Morozovska, Phys. Rev. B **104**, 174105 (2021).

[45] A. M. Gabovich, L. G. Il'chenko, and E. A. Pashitskii, Surf. Sci. **130**, 373 (1983).

[46] V. B. Shikin and Yu. P. Monarkha, *Two-Dimensional Charged Systems in Helium* (Nauka, Moscow, 1989), in Russian.

[47] *Two-Dimensional Electron Systems on Helium and Other Cryogenic Substrates*, edited by E. Y. Andrei (Kluwer Academic, Dordrecht, 1997).

[48] Yu. Z. Kovdrya, Fiz. Nizk. Temp. **29**, 107 (2003) [Low Temp. Phys. **29**, 77 (2003)].

[49] Y. Monarkha and K. Kono, *Two-Dimensional Coulomb Liquids and Solids* (Springer, New York, 2004).

[50] P. Leiderer, M. Wanner, and W. Schoepe, J. Phys. Colloques (Paris) **39**, C6-1328 (1978).

[51] C. F. Barenghi, C. J. Mellor, C. M. Muirhead, and W. F. Vinen, J. Phys. C: Solid State Phys. **19**, 1135 (1986).

[52] A. Kokalj and D. Costa, J. Electrochem. Soc. **168**, 071508 (2021).

[53] A. A. Kornyshev, D. J. Lee, S. Leikin, and A. Wynveen, Rev. Mod. Phys. **79**, 943 (2007).

[54] A. A. Kornyshev and A. Wynveen, Proc. Natl. Acad. Sci. USA **106**, 4683 (2009).

[55] R. G. Winkler and A. G. Cherstvy, in *Polyelectrolyte Complexes in the Dispersed and Solid State I. Principles and Theory*, edited by M. Müller (Springer, Berlin, 2014), pp. 1–56.

[56] S. A. M. Tofail and J. Bauer, Adv. Mater. **28**, 5470 (2016).

[57] D. M. Newns, Phys. Rev. B **1**, 3304 (1970).

[58] J. Heinrichs, Phys. Rev. B **8**, 1346 (1973).

[59] A. A. Kornyshev, A. I. Rubinshtein, and M. A. Vorotyntsev, Phys. Status Solidi B **84**, 125 (1977).

[60] R. Resta, Phys. Rev. B **16**, 2717 (1977).

[61] A. A. Kornyshev, A. I. Rubinshtein, and M. A. Vorotyntsev, J. Phys. C: Solid State Phys. **11**, 3307 (1978).

[62] A. M. Gabovich, L. G. Il'chenko, and E. A. Pashitskii, Fiz. Tverd. Tela **21**, 1683 (1979) [Sov. Phys. Solid State **21**, 965 (1979)].

[63] A. M. Gabovich, L. G. Il'chenko, E. A. Pashitskii, and Yu. A. Romanov, Surf. Sci. **94**, 179 (1980).

[64] M. A. Vorotyntsev and A. A. Kornyshev, Zh. Éksp. Teor. Fiz. **78**, 1008 (1980) [Sov. Phys. JETP **51**, 501 (1980)].

[65] L. G. Il'chenko, E. A. Pashitskii, and Yu. A. Romanov, Surf. Sci. **121**, 375 (1982).

[66] F. Bechstedt and R. Enderlein, Phys. Status Solidi B **131**, 53 (1985).

[67] A. M. Gabovich, V. M. Rosenbaum, and A. I. Voitenko, Surf. Sci. **186**, 523 (1987).

[68] J. Lindhard, Kgl. Danske Videnskab. Selskab. Mat.-Fys. Medd. **28**, 1 (1954).

[69] V. P. Silin and A. A. Rukhadze, *Electromagnetic Properties of Plasma and Plasma-Like Media* (Gosatomizdat, Moscow, 1961), in Russian.

[70] J. C. Inkson, J. Phys. C: Solid State Phys. **5**, 2599 (1972).

[71] R. R. Dogonadze and A. A. Kornyshev, J. Chem. Soc., Faraday Trans. II **70**, 1121 (1974).

[72] K. Schulze and K. Unger, Phys. Status Solidi (B) **66**, 491 (1974).

[73] A. A. Kornyshev, Electrochim. Acta **26**, 1 (1981).

[74] A. M. Gabovich and A. I. Voitenko, Phys. Status Solidi B **110**, 407 (1982).

[75] M. A. Vorotyntsev and A. A. Kornyshev, *Electrostatics of Media with Spatial Dispersion* (Nauka, Moscow, 1993), in Russian.

[76] V. M. Agranovich and V. L. Ginzburg, *Crystal Optics with Spatial Dispersion and Exciton Theory* (Springer, New York, 1984).

[77] L. D. Landau and E. M. Lifshits, *Electrodynamics of Continuous Media* (Nauka, Moscow, 1982), in Russian.

[78] E. H. Hwang and S. Das Sarma, Phys. Rev. B **75**, 205418 (2007).

[79] C. Freysoldt, P. Eggert, P. Rinke, A. Schindlmayr, and M. Scheffler, Phys. Rev. B **77**, 235428 (2008).

[80] M. Ghaznavi, Z. L. Mišković, and F. O. Goodman, Phys. Rev. B **81**, 085416 (2010).

[81] M. van Schilfgaarde and M. I. Katsnelson, Phys. Rev. B **83**, 081409(R) (2011).

[82] Z. L. Mišković, P. Sharma, and F. O. Goodman, Phys. Rev. B **86**, 115437 (2012).

[83] J. M. Pizarro, M. Rösner, R. Thomale, R. Valentí, and T. O. Wehling, Phys. Rev. B **100**, 161102(R) (2019).

[84] T. Sohier, M. Gibertini, and M. J. Verstraete, Phys. Rev. Materials **5**, 024004 (2021).

[85] W. R. Smythe, *Static and Dynamic Electricity* (McGraw-Hill, New York, 1950).

[86] A. Tugulea and D. Dascălu, J. Appl. Phys. **56**, 2823 (1984).

[87] M. Kumagai and T. Takagahara, Phys. Rev. B **40**, 12359 (1989).

[88] T. Sometani, Eur. J. Phys. **21**, 549 (2000).

[89] Y. L. Hao, A. P. Djotyan, A. A. Avetisyan, and F. M. Peeters, Phys. Rev. B **80**, 035329 (2009).

[90] H. Lin, Z. Xu, H. Tang, and W. Cai, J. Sci. Comput. **53**, 249 (2012).

[91] L. Wendler and B. Hartwig, J. Phys.: Condens. Matter **2**, 8847 (1990).

[92] A. M. Gabovich and A. I. Voitenko, J. Phys.: Condens. Matter **33**, 205002 (2021).

[93] P. Rivera, H. Yu, K. L. Seyler, N. P. Wilson, W. Yao, and X. Xu, Nat. Nanotechnol. **13**, 1004 (2018).

[94] J. D. Jackson, *Classical Electrodynamics* (Wiley, New York, 1998).

[95] R. H. Ritchie and A. L. Marusak, Surf. Sci. **4**, 234 (1966).

[96] D. M. Newns, J. Chem. Phys. **50**, 4572 (1969).

[97] A. V. Sidyakin, Zh. Éksp. Teor. Fiz. **58**, 573 (1970) [Sov. Phys. JETP **31**, 308 (1970)].

[98] J. W. Gadzuk, Surf. Sci. **23**, 58 (1970).

[99] D. E. Beck, V. Celli, G. Lo Vecchio, and A. Magnaterra, Nuovo Cimento **68**, 230 (1970).

[100] G. W. Ford and W. H. Weber, Phys. Rep. **113**, 195 (1984).

[101] J. Friedel, Philos. Mag. **43**, 153 (1952).

[102] B. N. J. Persson, J. Phys. C: Solid State Phys. **11**, 4251 (1978).

[103] B. N. J. Persson and M. Persson, Surf. Sci. **97**, 609 (1980).

[104] D. Dahal, G. Gumbs, and D. Huang, Phys. Rev. B **98**, 045427 (2018).

[105] A. M. Gabovich, M. S. Li, H. Szymczak, and A. I. Voitenko, J. Electrost. **102**, 103377 (2019).

[106] Y. Levin, Rep. Prog. Phys. **65**, 1577 (2002).

[107] A. Yu. Grosberg, T. T. Nguyen, and B. I. Shklovskii, Rev. Mod. Phys. **74**, 329 (2002).

[108] Y. Levin, J. Phys.: Condens. Matter **16**, S2149 (2004).

[109] F. Sciortino and P. Tartaglia, Adv. Phys. **54**, 471 (2005).

[110] R. H. French, V. A. Parsegian, R. Podgornik, R. F. Rajter, A. Jagota, J. Luo, D. Asthagiri, M. K. Chaudhury, Y.-M. Chiang, S. Granick, S. Kalinin, M. Kardar, R. Kjellander, D. C. Langreth, J. Lewis, S. Lustig, D. Wesolowski, J. S. Wettlaufer, W.-Y. Ching, M. Finnis *et al.*, Rev. Mod. Phys. **82**, 1887 (2010).

[111] A. Maciołek and S. Dietrich, Rev. Mod. Phys. **90**, 045001 (2018).

[112] X. Ji, X. Wang, Y. Zhang, and D. Zang, Rep. Prog. Phys. **83**, 126601 (2020).

[113] L. I. Boguslavsky, Prog. Surf. Sci. **19**, 1 (1985).

[114] V. S. Markin and A. G. Volkov, Prog. Surf. Sci. **30**, 233 (1989).

[115] L. I. Daikhin, A. A. Kornyshev, and M. Urbakh, J. Electroanal. Chem. **483**, 68 (2000).

[116] L. I. Daikhin, A. A. Kornyshev, and M. Urbakh, J. Electroanal. Chem. **500**, 461 (2001).

[117] A. A. Kornyshev, A. M. Kuznetsov, and M. Urbakh, J. Chem. Phys. **117**, 6766 (2002).

[118] Y. Tsori, Rev. Mod. Phys. **81**, 1471 (2009).

[119] J. B. Edel, A. A. Kornyshev, and M. Urbakh, ACS Nano **7**, 9526 (2013).

[120] J. B. Edel, A. A. Kornyshev, A. R. Kucernak, and M. Urbakh, Chem. Soc. Rev. **45**, 1581 (2016).

[121] K. Zhao and T. G. Mason, Rep. Prog. Phys. **81**, 126601 (2018).

[122] E. Hanamura, N. Nagaosa, M. Kumagai, and T. Takagahara, Mater. Sci. Eng. B **1**, 255 (1988).

[123] S. M. Badalyan and F. M. Peeters, Phys. Rev. B **85**, 195444 (2012).

[124] A. A. Kornyshev and M. A. Vorotyntsev, Surf. Sci. **101**, 23 (1980).

[125] G. Monet, F. Bresme, A. Kornyshev, and H. Berthoumieux, Phys. Rev. Lett. **126**, 216001 (2021).

[126] A. M. Gabovich and A. I. Voitenko, Eur. J. Phys. **39**, 045203 (2018).

[127] W. Thomson, in *The Cambridge and Dublin Mathematical Journal, Volume III*, edited by W. Thomson (Macmillan, Barclay, and Macmillan, Cambridge, 1848), pp. 141–148.

[128] I. S. Gradshteyn and I. M. Ryzhik, *Table of Integrals, Series and Products* (Academic, San Diego, CA, 2000).

[129] W. Li, X. Lu, S. Dubey, L. Devenica1, and A. Srivastava, Nat. Mater. **19**, 624 (2020).

[130] Yu. E. Lozovik and V. I. Yudson, Pis'ma Zh. Éksp. Teor. Fiz. **22**, 556 (1975) [JETP Lett. **22**, 274 (1975)].

[131] S. I. Shevchenko and I. O. Kulik, Pis'ma Zh. Éksp. Teor. Fiz. **23**, 171 (1976) [JETP Lett. **23**, 150 (1976)].

[132] O. L. Berman, G. Gumbs, and R. Y. Kezerashvili, Phys. Rev. B **96**, 014505 (2017).

[133] O. L. Berman and R. Y. Kezerashvili, Phys. Rev. B **96**, 094502 (2017).

[134] S. Saberi-Pouya, M. Zarenia, A. Perali, T. Vazifehshenas, and F. M. Peeters, Phys. Rev. B **97**, 174503 (2018).

[135] D. L. Duong, S. J. Yun, and Y. H. Lee, ACS Nano **11**, 11803 (2017).

[136] Y. Liu, Yu. Huang, and X. Duan, Nature (London) **567**, 323 (2019).

[137] M. Sammon and B. I. Shklovskii, Phys. Rev. B **99**, 165403 (2019).

[138] M. Florian, M. Hartmann, A. Steinhoff, J. Klein, A. W. Holleitner, J. J. Finley, T. O. Wehling, M. Kaniber, and C. Gies, Nano Lett. **18**, 2725 (2018).

[139] D. Erkensten, S. Brem, and E. Malic, Phys. Rev. B **103**, 045426 (2021).

[140] W. Jaskólski, Phys. Rep. **271**, 1 (1996).

[141] F. T. Vasko and A. V. Kuznetsov, *Electronic States and Optical Transitions in Semiconductor Heterostructures* (Springer, New York, 1999).

[142] G. Moody and S. T. Cundiff, Adv. Phys. X **2**, 641 (2017).

[143] M. T. Hossain and P. K. Giri, J. Appl. Phys. **129**, 175102 (2021).

[144] D. Van Tuan, M. Yang, and H. Dery, Phys. Rev. B **98**, 125308 (2018).

[145] L. Hao, Phys. Rev. B **104**, 195155 (2021).

[146] A. Chaves and F. M. Peeters, Solid State Commun. **334-335**, 114371 (2021).

[147] F. Bechstedt, P. Gori, and O. Pulci, Prog. Surf. Sci. **96**, 100615 (2021).

[148] M. A. Semina and R. A. Suris, Usp. Fiz. Nauk **192**, 121 (2022) [Phys. Usp. **65** (2022)].

[149] A. K. Geim and I. V. Grigorieva, Nature (London) **499**, 419 (2013).

[150] N. Ma and D. Jena, Phys. Rev. X **4**, 011043 (2014).

[151] K. S. Novoselov, A. Mishchenko, A. Carvalho, and A. H. Castro Neto, Science **353**, aac9439 (2016).

[152] J. Xiao, M. Zhao, Y. Wang, and X. Zhang, Nanophotonics **6**, 1309 (2017).

[153] N. Setter, D. Damjanovic, L. Eng, G. Fox, S. Gevorgian, S. Hong, A. Kingon, H. Kohlstedt, N. Y. Park, G. B. Stephenson, I. Stolitchnov, A. K. Taganstev, D. V. Taylor, T. Yamada, and S. Streiffer, J. Appl. Phys. **100**, 051606 (2006).

[154] W. Ding, J. Zhu, Z. Wang, Y. Gao, D. Xiao, Y. Gu, Z. Zhang, and W. Zhu, Nat. Commun. **8**, 14956 (2017).

[155] A. N. Morozovska, E. A. Eliseev, G. I. Dovbeshko, M. D. Glinchuk, Y. Kim, and S. V. Kalinin, Phys. Rev. B **102**, 075417 (2020).

[156] P. J. Feibelman, Prog. Surf. Sci. **12**, 287 (1982).

[157] A. M. Gabovich and A. I. Voitenko, Electrochim. Acta **28**, 1771 (1983).

[158] H. S. Harned and B. B. Owen, *The Physical Chemistry of Electrolytic Solutions* (Reinhold, New York, 1939).

[159] B. B. Smith and C. A. Koval, J. Electroanal. Chem. Interfacial Electrochem. **277**, 43 (1990).

[160] Y. Levin and J. E. Flores-Mena, Europhys. Lett. **56**, 187 (2001).

[161] Y. Levin, A. P. dos Santos, and A. Diehl, Phys. Rev. Lett. **103**, 257802 (2009).

[162] M. N. Tamashiro and M. A. Constantino, J. Phys. Chem. B **114**, 3583 (2010).

[163] D. Gillespie, M. Valiskó, and D. Boda, J. Chem. Phys. **155**, 221102 (2021).

[164] L. Wendler, F. Bechstedt, and M. Fiedler, Phys. Status Solidi B **159**, 143 (1990).

[165] E. A. Muljarov, S. G. Tikhodeev, N. A. Gippius, and T. Ishihara, Phys. Rev. B **51**, 14370 (1995).

[166] H. Zahra, A. Hichri, and S. Jaziri, J. Appl. Phys. **122**, 015701 (2017).